



1 **A new method for amino acid geochronology of the bivalve shell *Arctica***
2 ***islandica***

3 Martina L. G. Conti¹, Paul G. Butler², David J. Reynolds², Tamara Trofimova², James D. Scourse²,
4 Kirsty E. H. Penkman¹

5 ¹Department of Chemistry, University of York, York, YO10 5DD, United Kingdom

6 ²Centre For Geography And Environmental Science, University Of Exeter, United Kingdom

7 Correspondence to: Martina L.G. Conti (martina.conti@york.ac.uk)

8 **Abstract**

9 The bivalve mollusc *Arctica islandica* can live for hundreds of years, and its shell has provided a valuable resource for
10 sclerochronological studies and geochemical analyses for understanding palaeoenvironmental change. Shell specimens
11 recovered from the seabed need to be dated in order to aid sample selection, but existing methods using radiocarbon
12 dating or crossdating are both costly and time-consuming. We have investigated amino acid geochronology (AAG) as
13 a potential alternative means of providing a less costly and more efficient range-finding method. In order to do this, we
14 have investigated the complex microstructure of the shells, as this may influence the application of AAG. Each of the
15 three microstructural layers of *A. islandica* have been isolated and their protein degradation examined (amino acid
16 concentration, composition, racemisation and peptide bond hydrolysis). The intra-crystalline protein fraction was
17 successfully extracted following oxidation treatment for 48 h, and high temperature experiments at 140°C established
18 coherent breakdown patterns in all three layers, but the inner portion of the outer shell layer (iOSL) was the most
19 appropriate component due to practicalities. Sampling of the iOSL layer in Holocene shells from early and late
20 ontogeny (over 100-400 years) showed that the resolution of AAG is too low in *A. islandica* for within-shell age
21 resolution. However, analysis of 19 subfossil samples confirmed that this approach could be used to establish a relative
22 geochronology for this biomineral throughout the whole of the Quaternary. In the Late Holocene the temporal
23 resolution is ~1500-2000 years. Relative dating of 160 dredged shells of unknown age were narrowed down using
24 AAG as a range finder, showing that a collection of shells from Iceland and the North Sea covered the Middle Holocene,
25 Late Holocene, post-medieval (1171-1713 CE) and modern day. This study confirms the value of *A. islandica* as a
26 reliable material for range-finding and for dating Quaternary deposits.



27 **Short summary**

28 The mollusc *Arctica islandica* can survive for hundreds of years and its annual growth captures environmental
29 conditions, so each shell provides a detailed climatic record. Dating is essential for sample selection, but radiocarbon
30 and crossdating are time-consuming and costly. As an alternative, amino acid geochronology was investigated in the
31 three aragonitic layers forming the shells. This study confirms the value of AAG as a method for rangefinder dating
32 Quaternary *A. islandica* shells.

33 **1 Introduction**

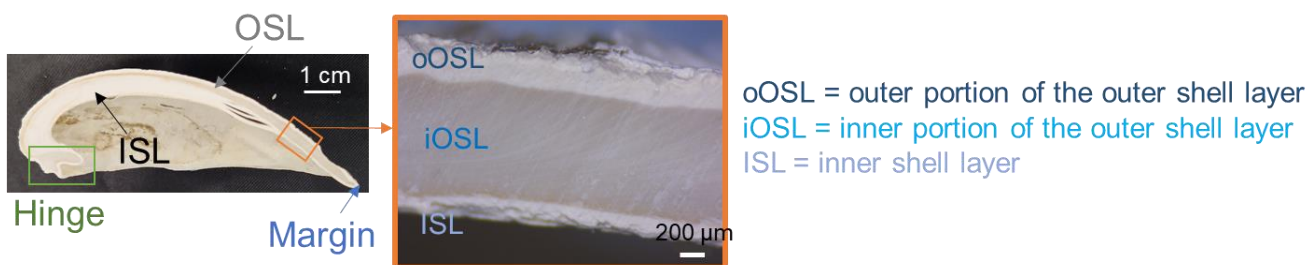
34 *Arctica islandica* (ocean quahog) is a bivalve mollusc that inhabits the continental shelf seas across the North Atlantic
35 region (MarLIN database). It presently lives across subpolar latitudes of the North Atlantic region of Europe from the
36 English Channel to the White Sea, and in North America from Virginia to Nova Scotia (MarLIN database, Schöne,
37 2013). Its Quaternary subfossil shells are also found in ancient sediments in Northern Europe and in the Mediterranean
38 Sea (Malatesta and Zarlenga, 1986; Eyles et al., 1994; Crippa et al., 2019). *Arctica islandica* has been routinely used
39 for palaeoclimate and palaeoceanographic studies due its exceptionally long life (>500 years maximum longevity;
40 Butler et al, 2013), and its capability to capture climatological changes within its periodic accretions (i.e. growth lines;
41 Witbaard et al., 1997; Schöne et al., 2005a; Schöne, 2013; Butler et al, 2013; Reynolds et al., 2016; Estrella-Martínez
42 et al., 2019). The study of annual and sub-annual band growth variability within the calcium carbonate shells, termed
43 sclerochronology, provides high-resolution detailed palaeoclimatology data spanning decades to multiple centuries
44 (Schöne et al., 2004; Schöne and Fiebig, 2008; Dunca et al., 2009; Butler et al., 2009, 2013; Wanamaker et al., 2012;
45 Reynolds et al., 2016; Trofimova et al., 2018; Estrella-Martínez et al., 2019; Brosset et al., 2022).

46 Developing sclerochronological records requires visual and statistical cross-matching across numerous samples; this
47 endeavour can be hugely time consuming and therefore needs to be targeted appropriately, especially when dead-
48 collected samples are of unknown age. Dating of the specimens is essential to develop accurate sclerochronological
49 records: radiocarbon dating can be a very precise technique for Late Quaternary marine shells (back to 40,000-55,000
50 years). However, this is not always economically viable (Hajdas et al., 2021), especially for a large number of samples,
51 while accurate correction for the marine reservoir effect is required and the dating uncertainty can be a few hundreds
52 of years (Alves et al., 2018). One possible alternative is amino acid geochronology (AAG), a relative-age technique
53 that is comparatively fast and inexpensive. AAG is applicable to mollusc shell deposits spanning the Quaternary period
54 (e.g. Sejrup and Haugen, 1994; Davies et al., 2009; Ortiz et al., 2009; 2015; Penkman, 2010; Demarchi et al., 2013a-
55 b, Bridgland et al., 2013), and can have high precision and resolution in tropical corals (Hendy et al., 2012).



56 AAG dating of biominerals is based on the natural degradation of proteins to determine age; the main processes are
57 racemisation (and epimerisation, both leading to an increase in amino acid D/L), peptide bond hydrolysis, and amino
58 acid decomposition (Hare and Mitterer, 1969). When organisms die, or when there is no more tissue turnover, these
59 degradation reactions occur in tandem. The inter-crystalline fraction of biominerals (Gries et al., 2009), the protein
60 which forms a matrix between the crystallites, is potentially more susceptible to external contamination or leaching,
61 and can compromise the reliability of AAG in some biominerals (Sykes et al., 1995, Penkman et al., 2008; Ortiz et al.,
62 2015). In some materials, a small fraction of the protein is contained within the interstitial voids of the crystal structure
63 and can be isolated with an oxidising pre-treatment; this is defined as the intra-crystalline (IcP) fraction (Towe and
64 Thompson, 1972; Sykes et al., 1995, Penkman et al., 2008; Gries et al., 2009). The IcP can be isolated with oxidation
65 using NaOCl (or H₂O₂ in some cases) and its stability against external contamination and leaching means that, in some
66 biominerals, it effectively operates as a closed-system. The isolation of closed-system IcP has provided reliable
67 chronological information in some gastropods (Penkman et al., 2008; Ortiz et al., 2015; Demarchi et al., 2013a-b;
68 Bridgland et al., 2013), ostracods (Ortiz et al., 2013), corals (Hendy et al., 2012; Tomiak et al., 2013; 2016), eggshell
69 (Brooks et al, 1990; Crisp et al., 2013), enamel (Dickinson et al., 2019; Baleka et al., 2021) and foraminifera (Wheeler
70 et al., 2021), but not in all biominerals (e.g. Orem and Kaufman, 2011; Torres et al., 2013; Demarchi et al., 2015).

71 A further complication for AAG of bivalve shells is that the different microstructural layers in bivalves are likely to be
72 composed of different proteins, and therefore may degrade differently. The *A. islandica* shell comprises a periostracum
73 and three aragonitic layers of differing crystal microstructure (Schöne, 2013): a homogeneous granular structure in the
74 outer portion of the outer shell layer (oOSL), a cross-acicular structure for the inner portion of the outer shell layer
75 (iOSL), and a cross-lamellar to cross-acicular structure for the inner shell layer (ISL; Fig. 1; Dunca et al., 2009; Schöne,
76 2013; Milano et al., 2017b).



77

78 Figure 1. (Left) cross section of *Arctica islandica* showing the (right) inner shell layer (ISL), inner portion of the outer
79 shell layer (iOSL), and outer portion of the outer shell layer (oOSL).



80 *Arctica islandica*, *Glycymeris glycymeris*, *Callista chione* and *Entemnotrochus adansonianus* have shown distinct
81 racemisation and epimerisation rates which depend on the microstructural layer analysed (Haugen and Sejrup, 1990,
82 1992; Sejrup and Haugen, 1994; Goodfriend et al., 1995, 1997; Torres et al., 2013; Demarchi et al., 2015). Early
83 studies without chemical oxidation on *A. islandica* (i.e. combining both the inter- and any intra-crystalline fraction)
84 showed different epimerisation rates, AA concentrations and composition between the inner and outer layers (Haugen
85 and Sejrup, 1990, 1992; Sejrup and Haugen, 1994). Intra-shell variability was also high, hypothesised to be due to
86 microorganism attack of the protein during early stages of diagenesis, external contamination and/or leaching through
87 micropores (Sejrup and Haugen, 1994; Kosnik and Kaufman, 2008). A study on the use of D/L for ontogenetic studies
88 of unbleached shells revealed Asp D/L values higher in the umbo growth lines (laid down when the shells are young)
89 compared to the rim growth lines (deposited when the shell is old; Goodfriend and Weidman, 2001). A difference in
90 AA composition between early and late ontogeny was also observed, indicating the need of sampling standardisation;
91 the recommendation was to sample shells from band year 20 in the outer shell layer (Goodfriend and Weidman, 2001).
92 Asx D/L values (Asx indicating aspartic acid and asparagine, that cannot be distinguished due to irreversible
93 deamination) in unbleached *A. islandica* shells collected between 1982 and 1994 were shown to increase with age over
94 a 154-year chronology, highlighting that AAG can potentially help in dating sclerochronologies (Marchitto et al.,
95 2000).

96 Given the variability observed in unbleached *A. islandica* shell AA data, a way forward is to test for the presence of
97 any IcP in *A. islandica* shells, and whether it forms a closed system for individual microstructures (e.g. Torres et al.,
98 2013; Demarchi et al., 2013a-b, 2015; Baldreki et al., 2024). The use of IcP in AAG has not been fully investigated
99 on *A. islandica* (Sykes et al., 1995), and there is variety in sampling strategy for specific microstructural layers (Haugen
100 and Sejrup, 1990, 1992; Sejrup and Haugen, 1994; Marchitto et al., 2000; Goodfriend and Weidman, 2001). If it is
101 possible to isolate an intra-crystalline fraction that exhibits closed-system behaviour from any of the layers in *A.*
102 *islandica* shells, an IcP approach may be able to reduce the intra-shell variability, and increase accuracy.

103 **1.1 Aims**

104 We present here a new method for the preparation of aragonitic *A. islandica* shells for AAG. To develop this
105 methodology, the following experiments were conducted:

- 106 - optimisation of the sampling method and isolation of the three microstructural layers (Sec. 2.2);
- 107 - assessment of aragonitic mineral diagenesis via X-ray diffraction (XRD) analysis (Sec. 3.1);
- 108 - testing for the existence of an intra-crystalline protein fraction via oxidation experiments (Sec. 3.2);



- 109 - testing for closed-system behaviour of *A. islandica* through controlled high temperature decomposition
110 experiments and assessment of the amino acid degradation patterns (Sec. 3.3);
- 111 - assessment of any change in amino acid composition and D/L values with ontogeny (Sec. 3.4);
- 112 - optimised method and recommendations for IcPD analysis of *A. islandica* (Sec. 3.5);
- 113 - analysis of multiple independently-dated subfossil shells to develop an initial AAG framework for *A. islandica*
114 in the North Atlantic Ocean (Sec. 3.6);
- 115 - age rangefinding of undated shells collected during research cruise DY150 of RRS *Discovery* in spring 2022
116 (Sec. 3.7).

117 **2 Materials and methods**

118 **2.1 *A. islandica* specimens**

119 In total, 19 *A. islandica* subfossil samples from the North Sea and Iceland were obtained for the bleaching and high
120 temperature experiments, ontogenetic trends and initial framework; these spanned in age from modern to ~2.1-2.2 Ma
121 and were independently dated with radiocarbon (^{14}C), AAG on other biominerals (see Table 1 for details; Fig. 2), and
122 sclerochronological crossdating (S; Table 1). In addition, 160 *A. islandica* shells of unknown age, incorporating
123 samples from both the North Sea and the North Icelandic shelf, were analysed for rangefinding (Sec. 3.7; Fig. 2).



124

125 Figure 2. Location of the *A. islandica* samples analysed in this work. Map created using © Google Earth.

126 Table 1. Overview of the *A. islandica* shells analysed in this study. Methods of dating: AAG: amino acid
 127 geochronology; ¹⁴C: radiocarbon; S: sclerochronologically crossdated. * Note: beach-collected samples could range
 128 thousands of years in age (e.g. Dominguez et al., 2016). § Further detail on radiocarbon dates are in Supplementary
 129 information Table S1. ※ Further information about sampling location are in Supplementary information Table S2.

Sample name	Number of shells and code	Locality	Latitude	Longitude	Estimated age	Independent previous dating	Reference for previous dating	Experiment
ArBrMod	n=1 N/A	Bridlington beach, UK	54° 4' N	0° 11' W	Modern?*, beach collected July 2021	N/A	N/A	pXRD (Sec. 3.1), framework (Sec. 3.6), rangefinding (Sec. 3.7)
ArPe, ArPe2	n=2 N/A	North Sea off Peterhead	58° 37' N	1° 27' E	Modern, live-collected, trawled at -114m depth in 2018	N/A	schnecken-und-muscheln.de	Bleaching (Sec. 3.2), high temperature (Sec. 3.3), framework (Sec. 3.6),



								range-finding (Sec. 3.7)
ArNsM1	n=1 0401381R	North Sea	59° 23.10' N	0° 31.00' E	1865-2004 CE	S	Butler et al., 2009	Ontogenetic trends (Sec. 3.4), framework (Sec. 3.6), range-finding (Sec. 3.7)
ArNsM2	n=1 0401422L	North Sea	59° 23.10' N	0° 31.00' E	1874-2004 CE	S	Butler et al., 2009	Ontogenetic trends (Sec. 3.4), framework (Sec. 3.6), range-finding (Sec. 3.7)
ArNsM3	n=1 0401423L	North Sea	59°23.10' N	0°31.00' E	1908-2004 CE	S	Butler et al., 2009	Ontogenetic trends (Sec. 3.4), framework (Sec. 3.6), range-finding (Sec. 3.7)
ArNs0246	n=1 0400246	North Sea	59° 7.5' N	0° 10.0' E	1867-2004 CE	S	Butler et al., 2009	pXRD (Sec. 3.1), ontogenetic trends (Sec. 3.4), framework (Sec. 3.6), range-finding (Sec. 3.7)
ArIcP2	n=1 061683M	Iceland	66° 31.59' N	18° 11.74' W	1397-1713 CE	S	Butler et al., 2013	Ontogenetic trends (Sec. 3.4), framework (Sec. 3.6), range-finding (Sec. 3.7)



ArIcP1	n=1 061682M	Iceland	66° 31.59' N	18° 11.74' W	1171-1391 CE	S	Butler et al., 2013	pXRD (Sec. 3.1), ontogenetic trends (Sec. 3.4), framework (Sec. 3.6), rangefinding (Sec. 3.7)
ArIc617	n=1 061617	Iceland	66° 31.59' N	18° 11.74' W	2841±33 ¹⁴ C yr BP 2545-2119 cal yr BP 2σ	¹⁴ C §	n/a §	Framework (Sec. 3.6), rangefinding (Sec. 3.7)
ArIc711	n=1 061711	Iceland	66° 31.59' N	18° 11.74' W	2938±33 ¹⁴ C yr BP 2678-2292 cal yr BP 2σ	¹⁴ C §	n/a §	Framework (Sec. 3.6), rangefinding (Sec. 3.7)
ArIc407	n=1 061407	Iceland	66° 31.59' N	18° 11.74' W	3411±37 ¹⁴ C yr BP 3223-2817 cal yr BP 2σ	¹⁴ C §	n/a §	Framework (Sec. 3.6), rangefinding (Sec. 3.7)
ArIc746	n=1 061746	Iceland	66° 31.59' N	18° 11.74' W	3535±36 ¹⁴ C yr BP 3364-2975 cal yr BP 2σ	¹⁴ C §	n/a §	Framework (Sec. 3.6), rangefinding (Sec. 3.7)
ArIc305	n=1 061305	Iceland	66° 31.59' N	18° 11.74' W	4222±40 ¹⁴ C yr BP 4257-3826 cal yr BP 2σ	¹⁴ C §	n/a §	Framework (Sec. 3.6), rangefinding (Sec. 3.7)
ArNs0658	n=1 010658	Fladen Ground (North Sea)	58° 50' N	0° 21.35' W	7810±25 ¹⁴ C yr BP 8340-8100 cal yr BP 2σ	¹⁴ C (Marine13 calibration)	Estrella-Martinez, 2019	Framework (Sec. 3.6), rangefinding (Sec. 3.7)
ArNsP1	n=1 10660	Fladen Ground (North Sea)	58.831° N	-0.356° E	7801±29 ¹⁴ C yr BP 8330-8070 cal yr BP 2σ	¹⁴ C (Marine13 calibration)	Estrella-Martinez, 2019	Ontogenetic trends (Sec. 3.4), framework (Sec. 3.6),



								range-finding (Sec. 3.7)
ArNsP2	n=1 10682	Fladen Ground (North Sea)	58.831° N	-0.356° E	7794±24 ¹⁴ C yr BP 8320-8060 cal yr BP 2σ	¹⁴ C (Marine13 calibration)	Estrella-Martinez, 2019	Ontogenetic trends (Sec. 3.4), framework (Sec. 3.6), range-finding (Sec. 3.7)
ArNsP3, ArNs0684	n=1 10684	Fladen Ground (North Sea)	58.831° N	-0.356° E	7752±23 ¹⁴ C yr BP 8280-8020 cal yr BP 2σ	¹⁴ C (Marine13 calibration)	Estrella-Martinez, 2019	pXRD (Sec. 3.1), ontogenetic trends (Sec. 3.4), framework (Sec. 3.6), range-finding (Sec. 3.7)
ArWey	n=1 N/A	Weybourne Crag, UK	52° 56.55' N	1° 08.33' E	Early Pleistocene (2.2-2.1 Ma)	AAG on <i>Bithynia</i> opercula and <i>Nucella</i> , biostratigraphic evidence	Preece et al., 2020	pXRD (Sec. 3.1), bleaching (Sec. 3.2), framework (Sec. 3.6)
Multiple names, see Table S2	n=73	Fladen Ground (North Sea)	Various ✖	Various ✖	Unknown	None	N/A	Range-finding (Sec. 3.7)
Multiple names, see Table S2	n=87	North Icelandic shelf	Various ✖	Various ✖	Unknown	None	N/A	Range-finding (Sec. 3.7)



131 **2.2 Sampling**

132 Each individual shell was sectioned from the umbo to the margin with an IsoMet 1000 precision cutter. After slicing, the
133 shells were sonicated in deionised water ($18.2 \text{ M}\Omega \text{ cm}^{-1}$) until no residue was observed (3 min, 2-3 washes). After air drying,
134 the periostracum (if present), was removed by drilling with an abrasive rotary burr on a hand-held rotary tool (Dremel drill).
135 Each layer (oOSL, iOSL and ISL; Fig. 1), was sampled by drilling using a Dremel drill equipped with a stainless-steel diamond-
136 coated drill bit with a small sphere or cylindrical tip. Following the experiments in sections 3.3 and 3.4, the iOSL layer was
137 chosen for building the AAG framework. To check changes in amino acids with ontogeny (e.g. with the biological age of the
138 shell; Sec. 3.4), the iOSL from early and late ontogeny within one shell (Table 1) was sampled: the former near the hinge and
139 the latter close to the ventral margin of the shell, likely containing a few annual growth increments. To build the AAG
140 framework (Sec. 3.7), intact Quaternary shells were subsampled near the margin of the shell where the iOSL was thickest.
141 Fragmented shells were sampled where the iOSL was thickest, for ease of sampling. Between each sample the drill tip was
142 cleaned in a 0.6 M HCl (Fisher, analytical grade) solution and MeOH (Fisher, HPLC grade) to reduce cross-contamination of
143 samples.

144 **2.3 Bleaching procedure**

145 Following protocols developed by Penkman et al., (2008), approximately 20-30 mg of powder was transferred to a 2 mL plastic
146 microcentrifuge tube (Eppendorf) and NaOCl (12 %, VWR, 50 $\mu\text{L mg}^{-1}$ of sample) was added. Samples were oxidised for 24-
147 72 h for bleaching experiments (Sec. 3.3). Following the results of these experiments, the iOSL layer of all other subfossil
148 samples was oxidised for 48 h. After the allotted time, the NaOCl was removed, and the powder was washed six times with
149 deionised water ($18.2 \text{ M}\Omega \text{ cm}^{-1}$) and once with MeOH (Fisher, HPLC grade). The samples were left to air dry for one to two
150 days.

151 **2.4 High temperature experiments**

152 High temperature experiments were carried out in a BinderTM ED23 oven set to 140 °C. To the bleached powder (10-20 mg),
153 300 μL of deionised water ($18.2 \text{ M}\Omega \text{ cm}^{-1}$) was added in a glass vial (Penkman et al., 2008). The samples were exposed to
154 high temperature conditions of 140 °C for 8, 24 and 48 h. After this time, the water was carefully removed and the powder
155 was left to air dry for 1-2 days.

156 **2.5 Isolation of free (FAA) and total hydrolysable amino acids (THAA)**

157 Following bleaching and in some cases high temperature exposure, the dry powder (1-10 mg) was split between free amino
158 acids (FAA) and total hydrolysable amino acids (THAA; Penkman et al., 2008). The FAA were demineralised in 2 M HCl



159 (10 $\mu\text{L mg}^{-1}$ of sample, minimum possible volume) and dried over a rotary vacuum concentration (Christ RVC 2-25 CDplus,
160 1300 rpm). The THAA samples were hydrolyzed in 7 M HCl (20 $\mu\text{L mg}^{-1}$ of sample) and heated at 110 $^{\circ}\text{C}$ for 24 h to
161 hydrolyse the peptide bonds. The samples were then dried in a rotary vacuum concentrator.

162 2.6 UHPLC-FLD analysis

163 Samples were rehydrated with a solution containing an internal standard - L-homo-arginine (0.01 mM), sodium azide (1.5
164 mM) and HCl (0.01 M) - to enable quantification of the amino acids. Analysis of chiral amino acid pairs was achieved using
165 an Agilent 1200 Series HPLC fitted with an Agilent Eclipse Plus C_{18} column (4.6 x 100 mm, 1.8 μm particle size) and
166 fluorescence detector (excitation wavelength = 230 nm, emission wavelength = 445 nm), using a UHPLC method modified
167 from Crisp (2013; Table 2). The binary mobile phase consisted of: (A) sodium acetate buffer (23 mM sodium acetate
168 trihydrate, sodium azide, 1.3 μM EDTA, adjusted to pH 6.00 \pm 0.01 with 10% acetic acid and sodium hydroxide), and (B)
169 92.5:7.5 methanol:acetonitrile. Table 2 reports the mobile phase, flow rate and temperature gradient of the separation. Data
170 processing was performed on ChemStation and data analysis on Excel; all data discussed in this paper is reported in
171 Supplementary information, Table S2. The Crisp (2013) method, is able to separate the L and D enantiomers of 14 amino
172 acids.

173 Table 2. Gradient of mobile phase, flow rate and column temperature for the UHPLC-FLD method. ‡ indicates that the
174 parameter does not change at the referred timepoint.

Time / min	% A / sodium acetate buffer	% B / 92.5:7.5 methanol:acetonitrile	Flow rate / mL min^{-1}	Column temperature / $^{\circ}\text{C}$
0.0	90	10.0	1.25	25
8.8	82.0	18.0	1.25	‡
10	82.0	18.0	1.25	28
11	82.0	18.0	1.25	28
23	78.3	21.7	1.25	28
25	78.3	21.7	1.25	28
32	75.2	24.8	1.25	28
34.5	74.0	26.0	1.25	28
36	65.0	35.0	1.25	28
50	‡	‡	1.30	25
56	50.0	50.0	1.30	25
62	2.0	98.0	1.30	25
67	95.0	5.0	1.25	25



175 **2.7 Powder XRD analysis**

176 Powder X-ray diffraction analysis was carried out on a selection of samples (Table 1) using a Bruker Panalytical Aeris Powder
177 XRD, scanned between 0-70° 2θ using a 0.2-degree increment per second. The scan axis was Gonio, source filter was Beta
178 nickel, beam mask was set to 20, beam knife to high, and antiscatter was 9 mm. The samples analysed were powdered either
179 by a rotary burr on a drill (section 2.2) or by homogenising to a fine powder with an agate pestle and mortar. Homogenised
180 *Cepea* spp. shells were used as aragonite standards and modern ostrich eggshell (OES) as calcite standard.

181 **3 Results and discussion**

182 The multilayer nature of *A. islandica* (comprising the oOSL, iOSL and ISL; Fig. 1) means that there are likely to be protein
183 differences between layers. This will dictate the original amino acid concentration and composition, and therefore their
184 diagenesis, with impacts on D/L values and AAG. Initially we present an assessment of the mineralogy (Sec. 3.1), followed
185 by the results from bleaching (Sec. 3.2) and heating experiments on the three microstructural layers (Sec. 3.3), assessing the
186 amino acid composition, concentration and D/L values. Ontogenetic trends on modern and subfossil shells are presented in
187 section 3.4. Recommendations for the method for AAG analysis of *A. islandica* (Sec. 3.5) are followed by an initial AAG
188 framework over the Quaternary period (Sec. 3.6), and application of the method to age ranging undated shells (Sec. 3.7).

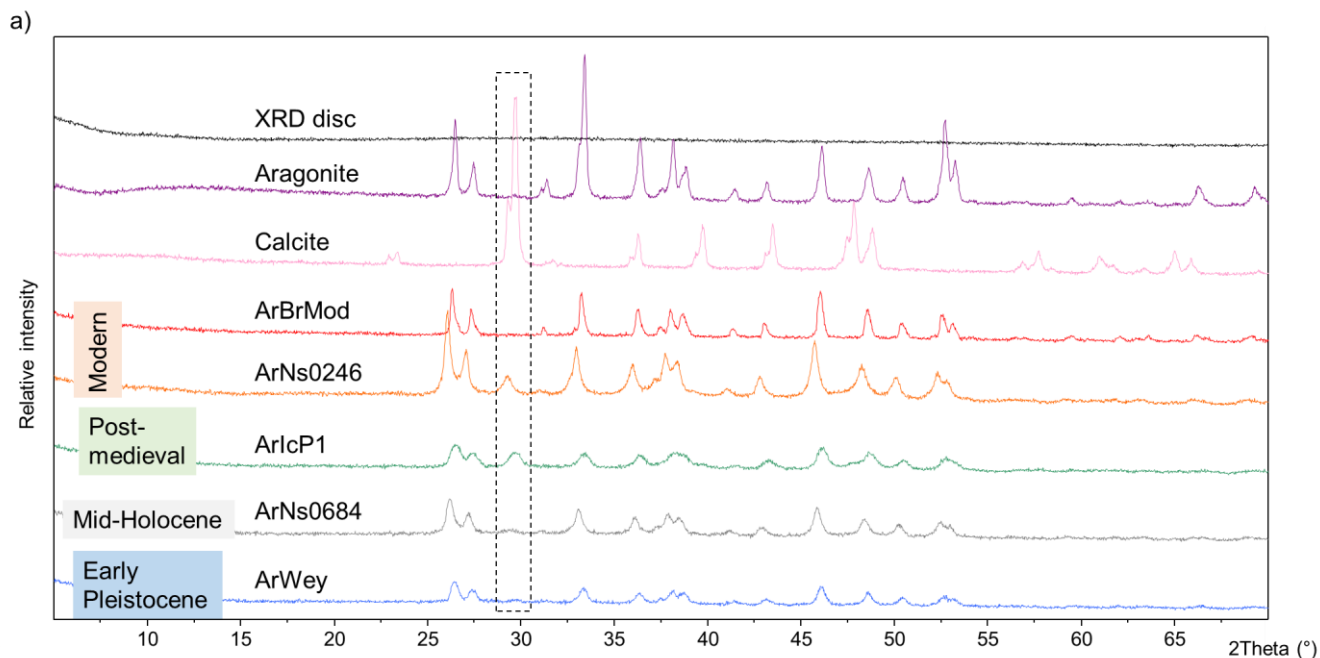
189 **3.1 Assessment of mineral diagenesis**

190 Aragonite, the polymorph of CaCO₃ that makes up the shells of *A. islandica*, can convert into calcite over geological timescales
191 or under stress (Brand and Morrison, 1987). The transition state in the transformation of labile aragonite into calcite can have
192 implications for the integrity of any closed system and the IcP (Preece and Penkman, 2005; Penkman, 2010). Thus,
193 investigating the mineral composition of samples may help to identify compromised samples; this can be done using X-ray
194 diffraction. In order to understand any potential changes to the CaCO₃ structure, powder XRD was carried out on a selection
195 of samples of a variety of ages to qualitatively assess the presence of aragonite and/or calcite (Table 1).

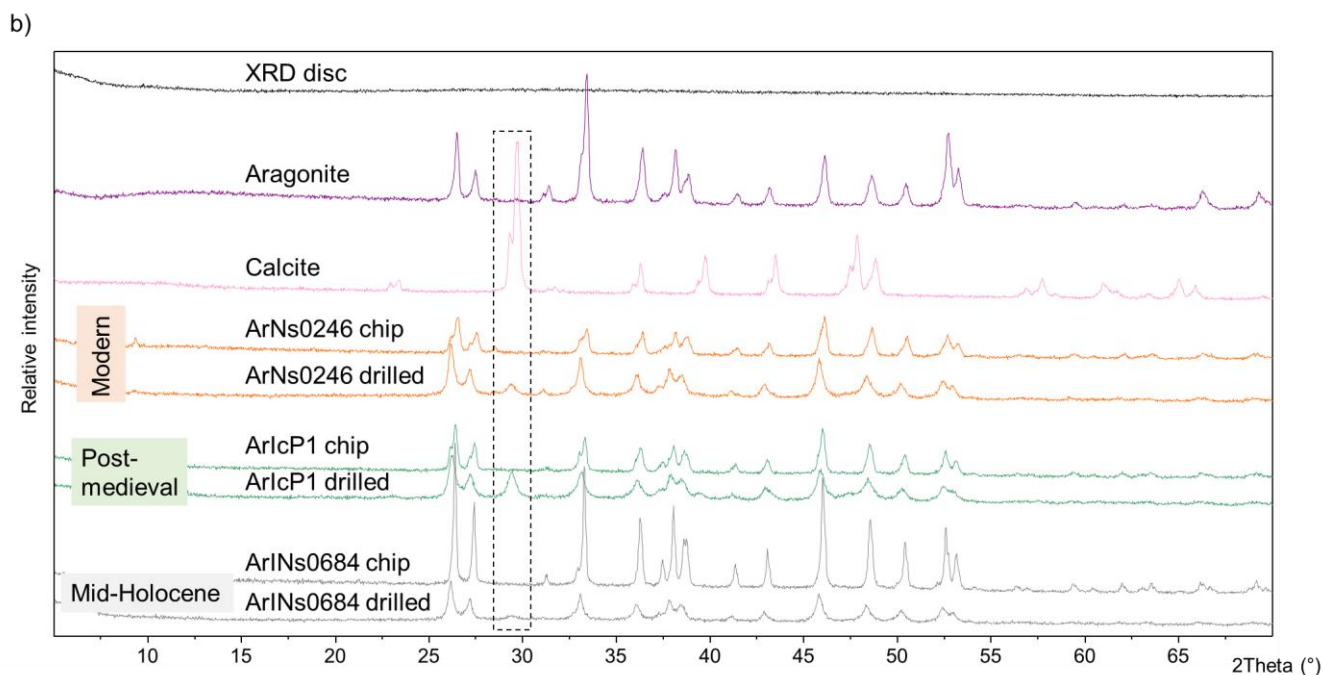
196 The diffractograms of modern (ArNs0246), medieval, Mid-Holocene (Walker et al., 2019) and Early Pleistocene shells that
197 were drilled show a small peak of calcite (theta 29°) in the mainly aragonitic shells (Fig. 3a). There is no clear pattern between
198 the age of the sample and the presence or absence of calcite; the Early Pleistocene shell (ArWey, 2.2-2.1 Ma) shows only a
199 very small calcite peak. It is possible that the abrasion and temperature created during the drilling process may affect the
200 aragonitic crystal structure (Báldreki et al., 2024). To test this, drilled powders were compared with shell chips from the same
201 samples homogenised with a pestle and mortar (Fig. 3b). The chips do not show a calcite peak at theta 29° (Fig. 3b); these
202 experiments indicate that the drilling process may cause some transformation of aragonite into calcite. However the drilling



203 process is necessary in order to remove the periostracum and isolate and sample the required layers for AAG. Therefore, it is
204 important to use the lowest speed possible and avoid applying extreme pressure when sampling using a rotary drill.



205



206

207 Figure 3. (a) pXRD spectra of *A. islandica* shells of various ages, powdered using a drill; (b) pXRD spectra of *A. islandica*
208 shells: in each case the same shell was drilled with a rotary burr (“drilled”), and homogenised with pestle and mortar (“chip”).
209 The dashed area in black represents the main peak of calcite at 2θ 29°. As the drilling process may convert aragonite into
210 calcite, it must be undertaken with care.

211 3.2 The impact of bleaching on amino acids

212 To test for any presence of an intra-crystalline protein fraction, bleaching experiments on each of the layers of *A. islandica* in
213 two shells (Table 1) was undertaken: a modern sample (ArPe) and an Early Pleistocene sample (ArWey).

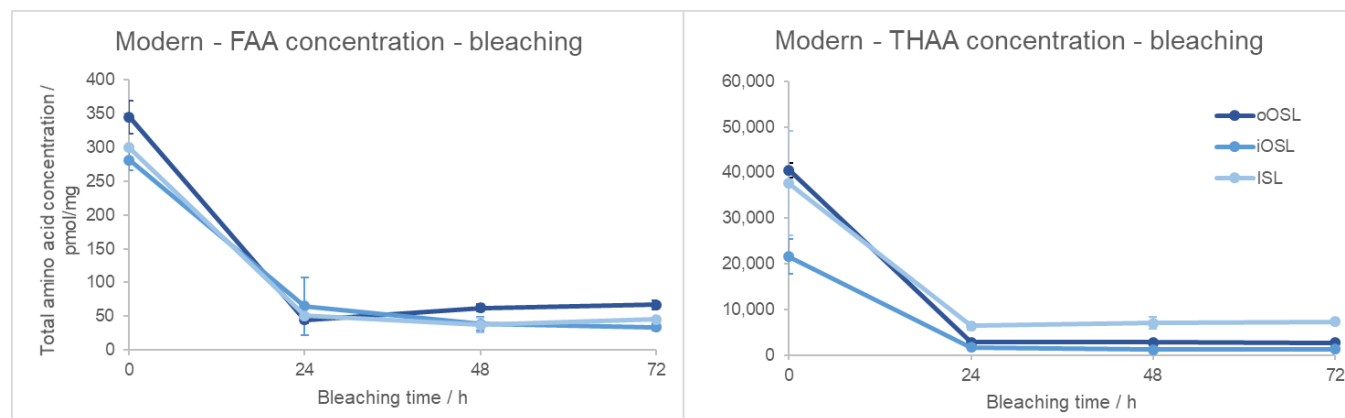
214 In the modern sample, the concentration of FAA and THAA in all layers decreases with bleaching (Fig. 4), meaning that an
215 inter-crystalline fraction is removed. There is an initial decrease and a subsequent very small increase in concentration after
216 24 h in the oOSL layer, possibly indicating that the prolonged bleaching process is breaking some of the peptide bonds,
217 increasing the concentration of amino acids from the intra-crystalline fraction. In the iOSL and ISL layers, the concentration
218 reaches a plateau between 48 and 72 h, indicating that an intra-crystalline fraction is more resistant to bleaching than the
219 unbleached shells and therefore requires long oxidation exposure. This isolated intra-crystalline fraction represents $17 \pm 3\%$
220 (all errors represent 1σ around the mean) of the oOSL, $16 \pm 5\%$ of the iOSL and $15 \pm 2\%$ of the ISL in the unbleached FAA
221 fraction. The total concentration in the FAA fraction is two orders of magnitude smaller than in the THAA fraction; as the



222 sample is young there would have been little natural breakage of the peptide bonds to form free amino acids. Following an
223 initial drop in concentration from 0-24 h, the concentration is stable in the THAA fraction with increasing bleaching time in
224 all layers. This intra-crystalline fraction represents $7 \pm 0.1\%$ of the oOSL and the iOSL ($\sigma=1$), and $18 \pm 1\%$ of the ISL in the
225 total unbleached THAA fraction. In summary, the FAA and THAA in the intra-crystalline fraction are stable and isolated
226 between 24-48 h in the modern *A. islandica* shell.

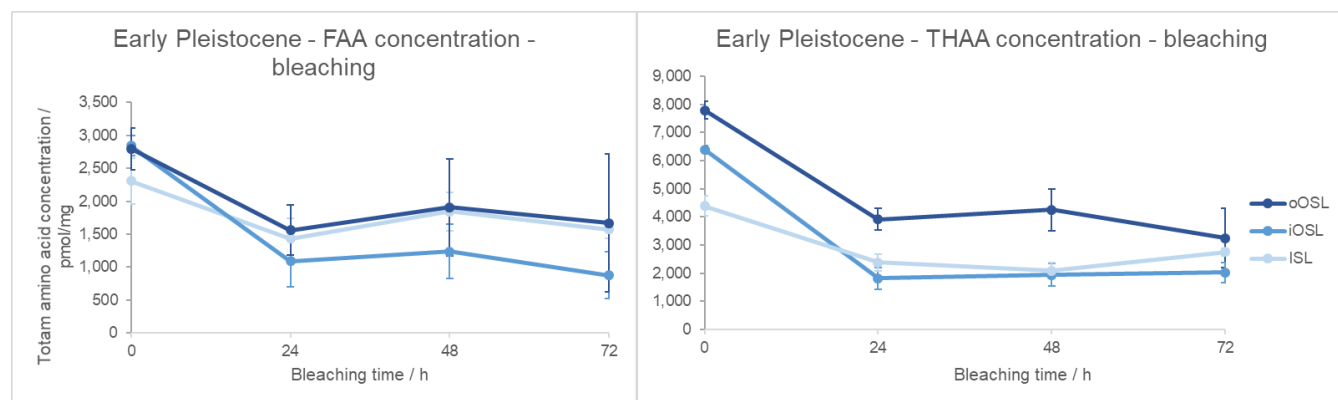
227 The geological formation of free amino acids through peptide bond hydrolysis is evident in the Early Pleistocene shell from
228 Weybourne Crag (Fig. 5). Similarly to the modern sample, the Early Pleistocene FAA and THAA decrease in concentration
229 with bleaching; the variability between replicates is larger so identification of the plateau is more challenging, potentially lying
230 between 48 h and 72 h in both the THAA and FAA fractions. Sykes et al. (1995) noted that solid slices of modern *A. islandica*
231 were less susceptible to 10% NaOCl oxidation compared to the shell powder - in the latter aspartic acid concentration reached
232 a plateau after 10 h - indicating that the intra-crystalline fraction for the powdered shell was isolated after just 10 h of oxidation.
233 In our study, when the individual shell layers are isolated and powdered, a concentration plateau is only achieved between 24
234 and 48 h (Fig. 5); in contrast to the results from Sykes et al. (1995), we therefore suggest that bleaching for 48 hours is necessary
235 to securely isolate the intra-crystalline protein fraction. In the Early Pleistocene shell, the percentage of intra-crystalline
236 fraction compared to the unbleached FAA fraction is $61 \pm 5\%$ in the oOSL, $38 \pm 5\%$ in the iOSL, and $70 \pm 7\%$ in the ISL; for
237 the THAA fraction the intra-crystalline fraction represents $49 \pm 5\%$ of the oOSL, $30 \pm 1\%$ of the iOSL, and $55 \pm 6\%$ of the
238 ISL. Due to the age of the shell, it is not surprising that the majority of the FAA are intra-crystalline, with the more labile
239 inter-crystalline free amino acids likely to have leached out of the system (Sykes et al., 1995). Despite the age of the shell
240 (~2.2-2.1 Ma), there are both inter- and intra-crystalline amino acids present (Demarchi, 2009; Penkman et al., 2011; Demarchi
241 et al., 2013a-b; Ortiz et al., 2015, 2018). It is interesting to note that the ISL and oOSL layers contain a higher relative
242 percentage of intra-crystalline protein (oOSL = $49 \pm 5\%$, ISL = $55 \pm 6\%$), whereas the iOSL has a much lower proportion of
243 IcP ($30 \pm 1\%$).

244



245

246 Figure 4. Decrease in total amino acid concentration upon bleaching modern *Arctica islandica* (from the North Sea off
247 Peterhead, UK) for the oOSL, iOSL and ISL microstructural layers. Error bars indicate one standard deviation about the mean
248 based on three replicates. Note the large drop in concentration with bleaching, with a plateau reached by 48 h.



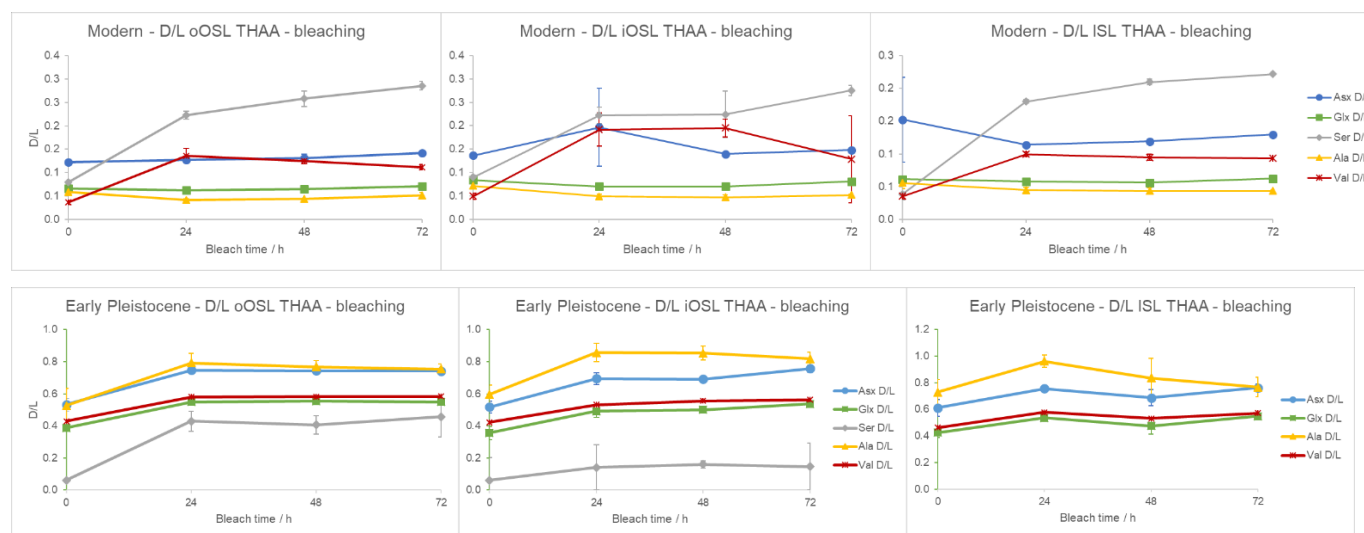
249

250 Figure 5. Change in total amino acid concentration upon bleaching Early Pleistocene *A. islandica* (from Weybourne Crag, UK)
251 for the oOSL, iOSL and ISL microstructural layers. Error bars indicate one standard deviation about the mean based on two
252 replicates. Note the drop in concentration with bleaching with a plateau reached by 48 h.

253 As the oxidation step has been shown to induce some racemisation in other mollusc shells, especially with long exposure
254 (Penkman et al., 2008), when choosing the optimal bleaching time both concentration and racemisation have to be considered.
255 In the modern and Early Pleistocene samples there is an initial increase in D/L for Asx (aspartic acid), Glx (glutamic acid),
256 Ser (serine), Ala (alanine) and Val (valine) between 0-24 h bleaching, indicating that the removal of the inter-crystalline protein
257 leaves more racemised amino acids in the IcP (Penkman et al., 2008). The D/L values reach a plateau between 24 h and 48 h,
258 and at the 72 h timepoint the D/L values slightly increase for most amino acids, suggesting that some oxidation-induced



259 racemisation is taking place (Fig. 6). Nevertheless, the concentration plateau reached at 48 h in both the modern and Early
260 Pleistocene samples and the small change in D/L values indicates that the intra-crystalline protein fraction is effectively stable
261 and relatively protected from oxidation.



262

263

264 Figure 6. Mean THAA D/L of Asx, Glx, Ser, Ala & Val in *A. islandica* upon bleaching for the oOSL, iOSL and ISL
265 microstructural layers. Top: modern shell from Peterhead; error bars indicate one standard deviation based on three replicates.
266 Bottom: Early Pleistocene shell from Weybourne Crag; error bars indicate one standard deviation based on two replicates.
267 There is an initial increase in D/L with bleaching, but stable D/L with prolonged bleaching.

268 The percentage composition of each amino acid in the bleached and unbleached samples can provide information about the
269 nature of protein in the two fractions, if different. The composition of the unbleached shell and IcP is similar for the THAA
270 fraction, but some differences are present in the FAA fraction in the modern sample (Fig. 7, Supplementary information Fig.
271 S1). In this fraction, in the bleached samples Gly (glycine) is much higher and Ser, Ala and Arg (arginine) are lower; however
272 this may be due to the very low concentrations of minor amino acids, sometimes below the limit of detection. In the Early
273 Pleistocene sample, the composition is very similar between the unbleached and bleached fractions in both the FAA and THAA
274 (Supplementary information Fig. S2), confirming that the majority of amino acids in the unbleached samples are intra-
275 crystalline, and that much of the inter-crystalline protein fraction has leached out with time.

276 In addition to differences in amino acid concentration between the three layers of *A. islandica*, there are also slight differences
277 in composition between layers. In the THAA fraction of the modern shell bleached for 48 h, all three layers have similar
278 composition, with some exceptions: Ala is higher in the iOSL and Arg is lower in the ISL than in the other two layers. The
279 percentage composition of Gly is slightly higher in the oOSL than the iOSL and ISL, although the between-sample variability



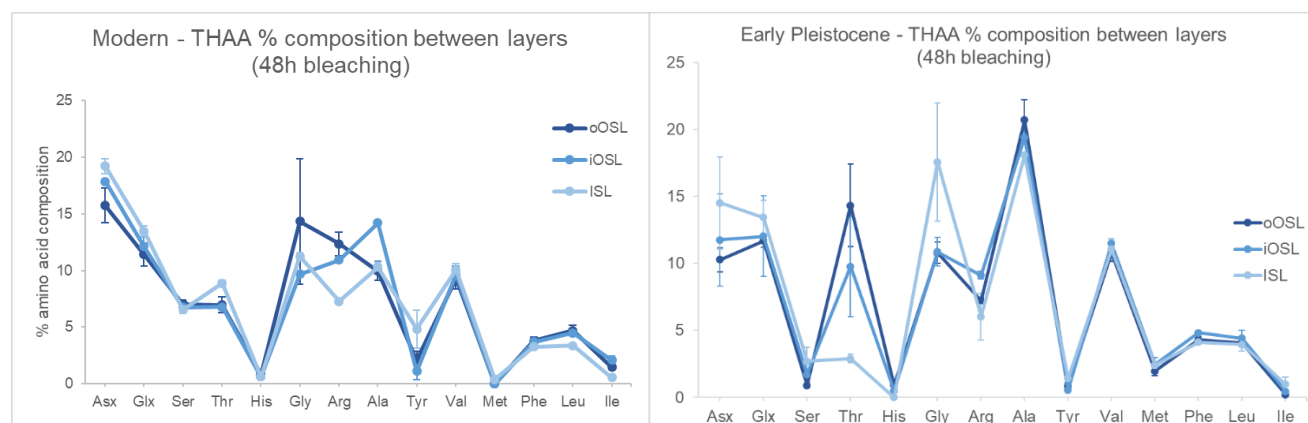
280 is larger than for the other two layers which may confound the results (Fig. 7). In the Early Pleistocene shell, the FAA fraction
281 shows very similar composition between the three layers. In the THAA fraction, the ISL and iOSL contain higher amounts of
282 Asx and Glx, while Thr (threonine) is more abundant in the two OSL layers and Gly is highest in the ISL layer. There is
283 mostly agreement in the composition of the two shells. The higher percentage composition of Gly in the Early Pleistocene
284 shell is likely to be due to the natural diagenesis of Val (valine), Ser, Thr and Tyr (tyrosine) to form Gly (Vallentyne, 1964).
285 Ser is much lower and Ala higher in the Early Pleistocene samples: Ser is thermally unstable and can degrade to form Ala and
286 Gly (Vallentyne, 1964; Bada et al., 1978), while Ala can be a product of dehydration of Ser and Asx (Walton, 1998). The
287 overall differences in amino acid composition in both modern and Early Pleistocene shells for the three layers shows that
288 originally there are different proteins in the layers, which then break down at different rates; therefore, it is important to
289 consistently sample one layer for reliable AAG.

290 Haugen and Sejrup (1990) presented the percentage composition of 30 modern unbleached specimens of *A. islandica* for both
291 the inner and outer shell layers; as there was no separation into oOSL and iOSL, their results for the ‘outer’ layer are compared
292 to our oOSL and iOSL results (Supplementary information Fig. S1b). Additionally, Haugen and Sejrup (1990) analysed their
293 amino acid with ion-exchange chromatography rather than HPLC, and they do not report His (histidine), Arg and Met
294 (methionine). The percentage composition of the FAA and THAA fractions from the modern shell analysed here and the 30
295 shells from Haugen and Sejrup (1990) are very similar, with only small variations (Supplementary information Fig. S1b). In
296 the FAA fraction there is a lower contribution from Tyr in our data (3-4%) compared to 13-15% in the Haugen and Sejrup
297 (1990) shells, while Gly is higher in our data for the bleached shells (44-67%), but more comparable in the unbleached samples
298 (our work = 31-34%, Haugen and Sejrup, 1990 = 21-24%). In the THAA fraction the percentage composition from Haugen
299 and Sejrup (1990) are within error with our bleached data, while our unbleached shell has higher Gly and lower Asx and Glx.
300 There is remarkable similarity in percentage composition between Haugen and Sejrup (1990) results without bleaching and
301 our modern bleached shells; this may ultimately enable the comparison between data from samples analysed prior to and after
302 establishing the bleaching step in the AAG method.

303 A recent study compared the percentage composition of amino acids in untreated and oxidised modern shells, including 12%
304 NaOCl treatment on powdered shell where the layers had been homogenised (Huang et al., 2023). Similar to our results, Gly,
305 Asx and Glx were the dominant amino acids in the unbleached shells, followed by Ala, Ser and Thr (Supplementary
306 information Fig. S1a). Upon bleaching, Pro (proline) was the most abundant amino acid (Huang et al., 2023), but this
307 secondary amino acid is not quantified in the current analytical method used for AAG. As in our bleaching experiments, in
308 the work of Huang et al. (2023) upon bleaching Gly decreased in composition, while Asx, Glx, Ala, Val, Arg, Phe showed an
309 increase in composition; other amino acids present in lower concentrations show no or opposite trend. There is therefore a
310 general agreement between the study from Huang et al. (2023) and our current work, with the differences possibly due to the



311 sampling approach: Huang et al. (2023) homogenised all three aragonitic layers after removing the periostracum, whereas our
312 study separates the oOSL, iOSL and ISL, providing a more detailed study of the amino acid composition in the three
313 microstructural layers.



314
315 Figure 7. Mean THAA percentage composition in the three microstructural layers of *A. islandica* from (left) a modern sample
316 from Peterhead, and (right) an Early Pleistocene shell from Weybourne Crag. Error bars represent one standard deviation
317 based on three replicates for the shell from the modern shell, and two replicates from the Early Pleistocene shell. There are
318 differences in amino acid composition between the three aragonitic layers in the modern and Early Pleistocene shells,
319 indicating differences in original protein composition.

320 3.3 Elevated temperature experiments to test for closed system behaviour

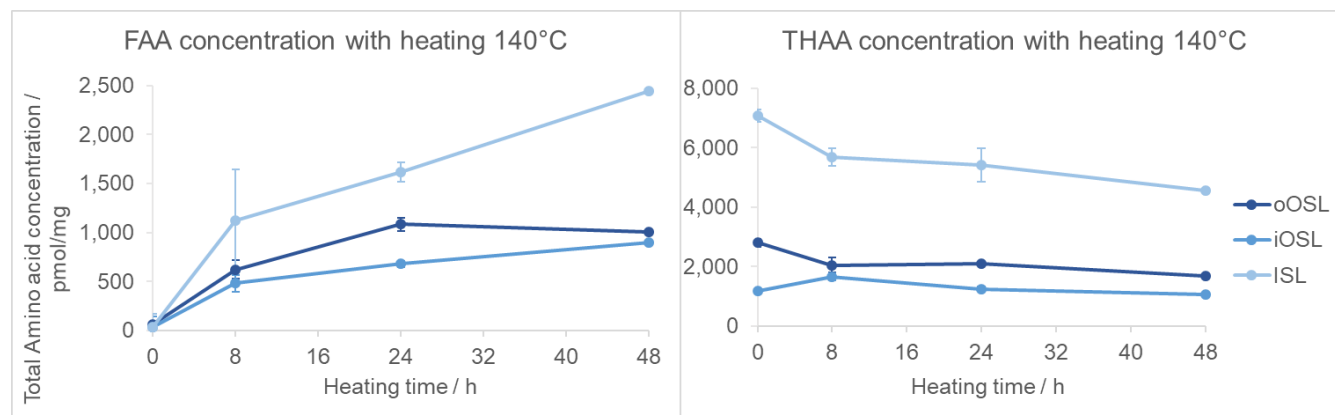
321 High temperature experiments are considered a controlled, simple way to assess the suitability of biomineral proteins for AAG
322 (Kriausakul and Mitterer, 1978; Haugen and Sejrup, 1992; Penkman et al., 2008; Hendy et al., 2012; Demarchi et al., 2013).
323 The resistance of the IcP to oxidation was shown with bleaching experiments on modern and Pleistocene shells (Sec 3.2). To
324 test whether the IcP behaves like a closed system, the bleached powder (48 h) from the three layers of a modern shell of *A.*
325 *islandica* from the North Sea (ArPe, Table 1) was exposed to high temperatures in hydrous conditions (140°C for 8, 24, 48 h),
326 and the protein degradation (including rates of racemisation) observed. The high temperature experiments are utilised to
327 accelerate the protein degradation and explore the processes that would otherwise occur over thousands of years. Previous
328 studies showed that the degradation patterns in high temperature heating experiments do not necessarily produce the same
329 degradation patterns in subfossil samples; low temperature data (~80°C) may be more similar to subfossil results but requires
330 long exposure (Crisp et al., 2013; Tomiak et al., 2013; Demarchi et al., 2013). Nevertheless, the chosen temperature of 140°C
331 allows for quick assessment of protein degradation patterns and leaching over short timescale (a few days), while trends in



332 concentration and D/L values, and correlations of FAA and THAA D/L with increased exposure to 140°C can provide evidence
333 on whether the amino acids in *A. islandica* behave as a closed-system (Penkman et al., 2008).

334 The total concentration of FAA in the intra-crystalline fraction increases over time because prolonged heating breaks the
335 peptide bonds to ultimately release free amino acids (Fig. 8). The total THAA concentration decreases with heating due to the
336 decomposition of amino acids (Penkman et al., 2008; Crisp et al., 2013; Tomiak et al., 2013; Demarchi et al., 2013), discussed
337 in detail below. An interesting observation is that the ISL layer has a higher THAA concentration than the other layers, but
338 also has a steep increase in FAA concentration with heating time, coinciding with a steep drop in THAA concentration. This
339 means that the amino acids in the inner layer (ISL) are more susceptible to peptide bond hydrolysis, and in the hydrolysable
340 fraction (which includes both bound and free AAs), they are more prone to decomposition than the outer layer. This may be
341 due to differences in the proteins' primary sequence or higher structures, or a result of the way the proteins are mineral-bound
342 in the ISL microstructure. Conversely, the concentration of FAA and THAA in the iOSL layer shows the least change,
343 indicating that the protein in this layer may be more resistant to degradation.

344 The different rates of breakdown of the three layers indicate the importance of consistently sampling one microstructure for
345 obtaining more reliable AAG results.



346
347 Figure 8. FAA and THAA concentration changes with heating at 140°C in the three shell layers of modern *A. islandica*. Error
348 bars indicate one standard deviation based on three replicates. The FAA concentration increases with heating due to peptide
349 bond hydrolysis; the ISL seems to have faster peptide bond hydrolysis compared to the other layers.

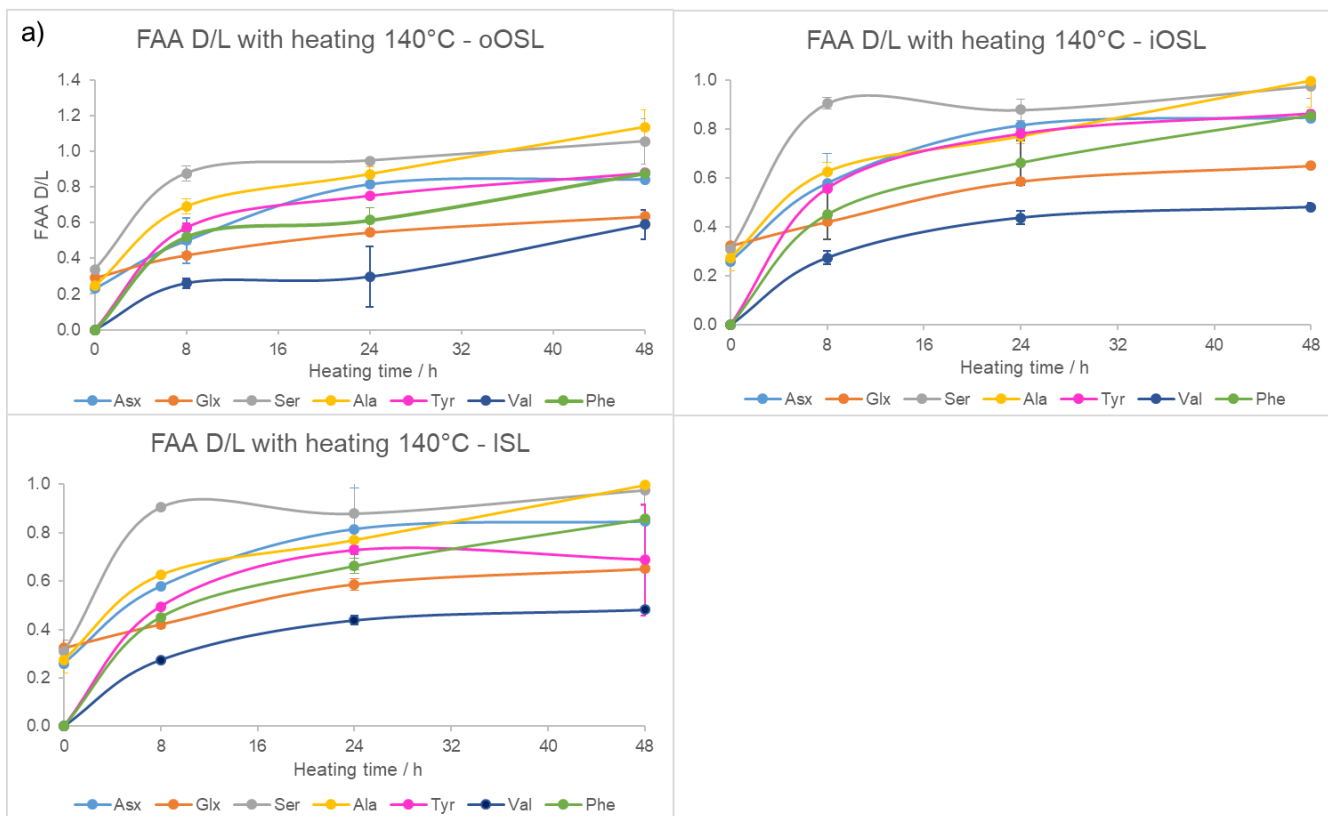
350 If *A. islandica* resembles a closed system the diagenetic products of protein degradation would be retained, and thus the FAA
351 and THAA D/L would be highly correlated (Preece and Penkman, 2005; Penkman et al., 2007; Demarchi et al., 2011, 2015).
352 As expected, the D/L values for all amino acids increase with increased heating duration in all layers (Fig. 9a, Supplementary



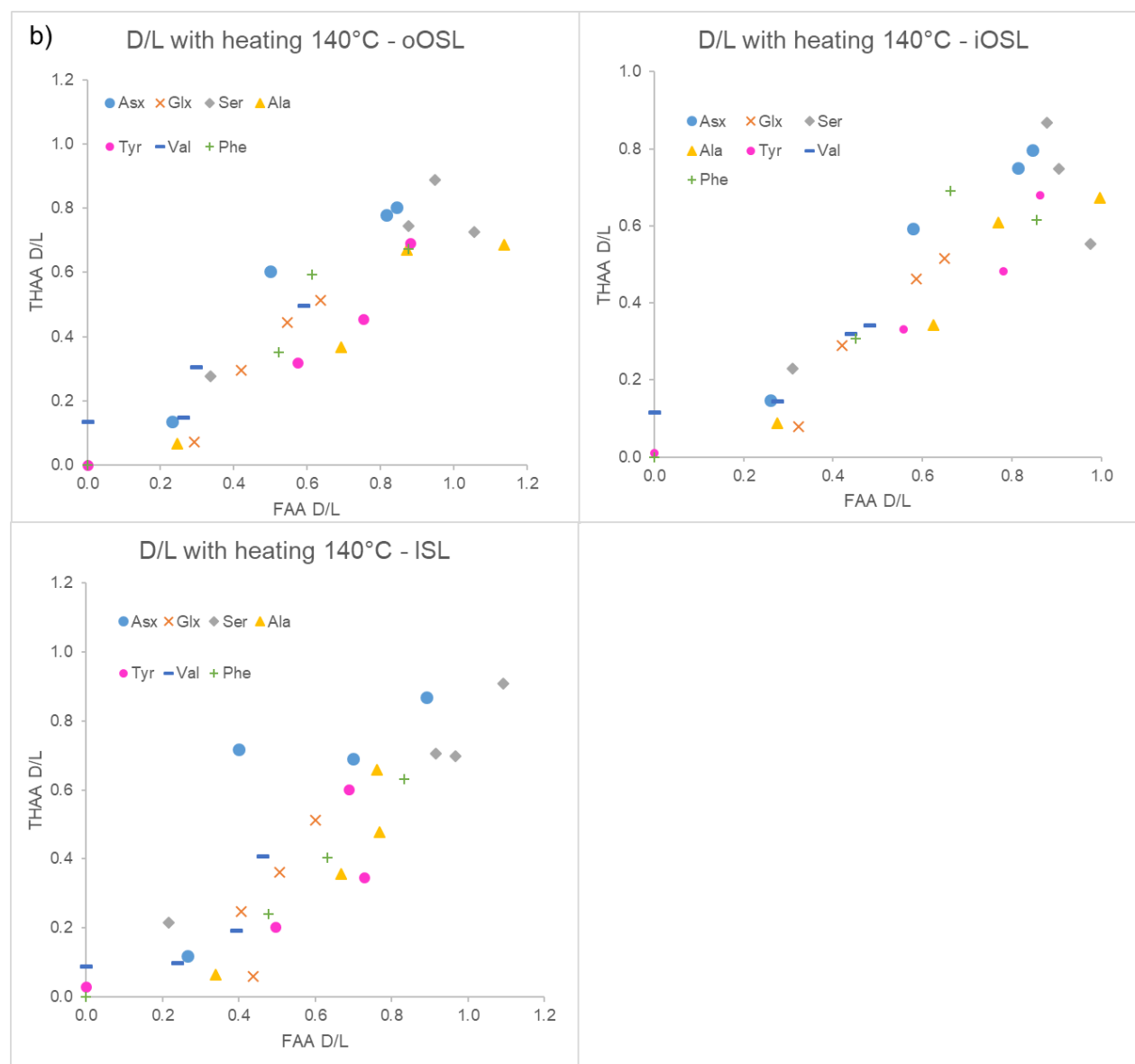
353 information Fig. S3) meaning that racemisation patterns follow reliable trends in the intra-crystalline protein fraction in *A.*
354 *islandica*. Figure 9b shows the correlation of FAA and THAA for Asx, Glx, Ser, Ala, Tyr, Val and Phe: overall, all amino
355 acids from all layers show high covariance indicative of closed-system behaviour. However, some scattering is observed for
356 the ISL layer. There is also some scattering for Ser especially in the outer layers, which is expected in these high temperature
357 experiments (Bright and Kaufman, 2011; Crisp et al., 2013) because the thermally unstable Ser (the “parent”) readily degrades
358 into Gly and Ala (the “products”). It is expected that the ratio of the “parent” over a degraded product will decrease with
359 heating and thus indicate increased decomposition (Bada et al., 1978). This is particularly evident after 8 h heating with a
360 marked reduction in the ratio of [Ser]/[Ala] (Fig. 10). In the THAA fraction Ser D/L decreases after 24 h (Supplementary
361 information Fig. S4) due to decomposition of free serine, resulting in a decrease in the overall racemisation of Ser (Penkman,
362 2010).

363 Other decomposition pathways include the degradation of Ser, Thr and Tyr (the “parent”) into Gly (Vallentyne, 1964), and
364 Asx (the “parent”) into Ala (Walton, 1998). These trends were observed in all cases in the FAA and THAA samples of the
365 iOSL layer after 8 h and in the oOSL layer after 24 h, whereas in the ISL layer the ratios increased in some cases
366 (Supplementary information Fig. S4). As previously mentioned for the concentration and D/L values, this could either be due
367 to how the different peptides are bound to the mineral, or differences in protein sequence and structure in the ISL layer
368 compared to the outer layers. Upon heating, the concentration of FAA increases at a high rate in the ISL (Fig. 8) and the steep
369 “parent”-product ratios may reflect the more labile nature of the peptide bonds. The THAA composition of the bleached
370 unheated ISL layer also shows a higher percentage of the more labile “parent” amino acids Asx, Thr and Tyr compared to the
371 outer layers, while Ser has similar composition in all three layers (Supplementary information Fig. S5). Therefore, the high
372 proportion of amino acids with labile peptide bonds in the ISL explains the high decomposition rate of FAA (Fig. 8) and the
373 faster degradation rates.

374 The high correlation between FAA and THAA amino acid D/L values and the predictable degradation pattern observed from
375 the high temperature experiments point towards a closed-system behaviour for *A. islandica* in all three layers. However, these
376 differences in rates of degradation between the inner and outer layers would affect the D/L values and the accuracy of the AAG
377 interpretation, therefore it is preferable to analyse one specific layer. Interestingly, in the ISL a high proportion of amino acid
378 is lost to hydrolysis in the THAA fraction and to degradation in the FAA fraction. In isotope studies the oOSL is not used
379 because it can be more readily contaminated or impacted by environmental factors, it being the most external layer (Schöne,
380 2013). The iOSL is routinely used in isotope analyses and can be used in sclerochronology (Schöne and Huang, 2021; Butler
381 et al., 2009). Due to the previous research on the iOSL, our bleaching and high temperature degradation experiments and ease
382 of sampling the iOSL, we therefore suggest using this same layer for AAG.

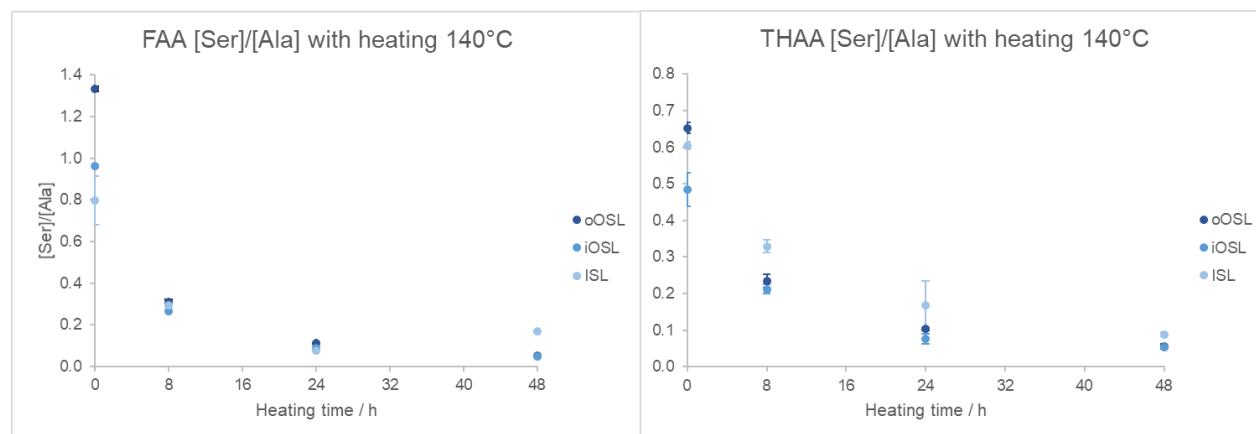


383



384

385 Figure 9. (a) Mean FAA D/L with increased duration of heating at 140°C in the three bleached layers of modern *A. islandica*; error
386 bars indicate one standard deviation based on three replicates. (b) FAA vs. THAA D/L with heating at 140°C. D/L values increase
387 with increasing exposure to high temperature in all three aragonitic layers, and high correlation between the FAA and THAA
388 fractions in most cases.



389

390 Figure 10. [Ser]/[Ala] in the bleached oOSL, iOSL and ISL layers of modern *A. islandica* from Peterhead following heating
391 at 140°C for 8-48 h. Error bars indicate one standard deviation based on three replicates. The [Ser]/[Ala] decreases with
392 heating in all three aragonitic layers.

393 3.4 Assessing ontogenetic trends in modern and subfossil AAG

394 Previous work on amino acid $\delta^{15}\text{N}$ of *A. islandica* has shown changes in isotope values and amino acid composition with
395 ontogeny, i.e. with biological age of the shell (Schöne and Huang, 2021). Here, eight shells with known ages spanning 100-
396 400 years (Table 1) were sampled near the hinge (representing the early ontogenetic age of the shell) and near the margin
397 (representing late ontogeny), to check for any differences in composition and D/L values. Given the importance of original
398 protein composition to the subsequent degradation, it is important to determine whether there are differences in concentration
399 and D/L between early and late ontogeny as seen in amino acid isotopic analyses (Schöne and Huang, 2021). In addition, if
400 the rates of the reactions are fast enough, it may be possible to use AAG for age resolution *within* an individual shell. For
401 example AAG has been used in sclerochronological studies of tropical *Porites* corals (e.g. Goodfriend et al., 1992), providing
402 a resolution of ± 6 years in most recent material and ± 24 years in the last 150 years (Hendy et al., 2012). In those cases the
403 ability to obtain high resolution data was due to the relatively high ambient temperatures ($\sim 26^\circ\text{C}$; Hendy et al., 2012) in which
404 the corals live, but the lower temperatures of *A. islandica*'s habitat ($\sim 1\text{-}16^\circ\text{C}$; Schöne, 2013) mean that AAG for
405 sclerochronology may not be applicable to this biomineral.

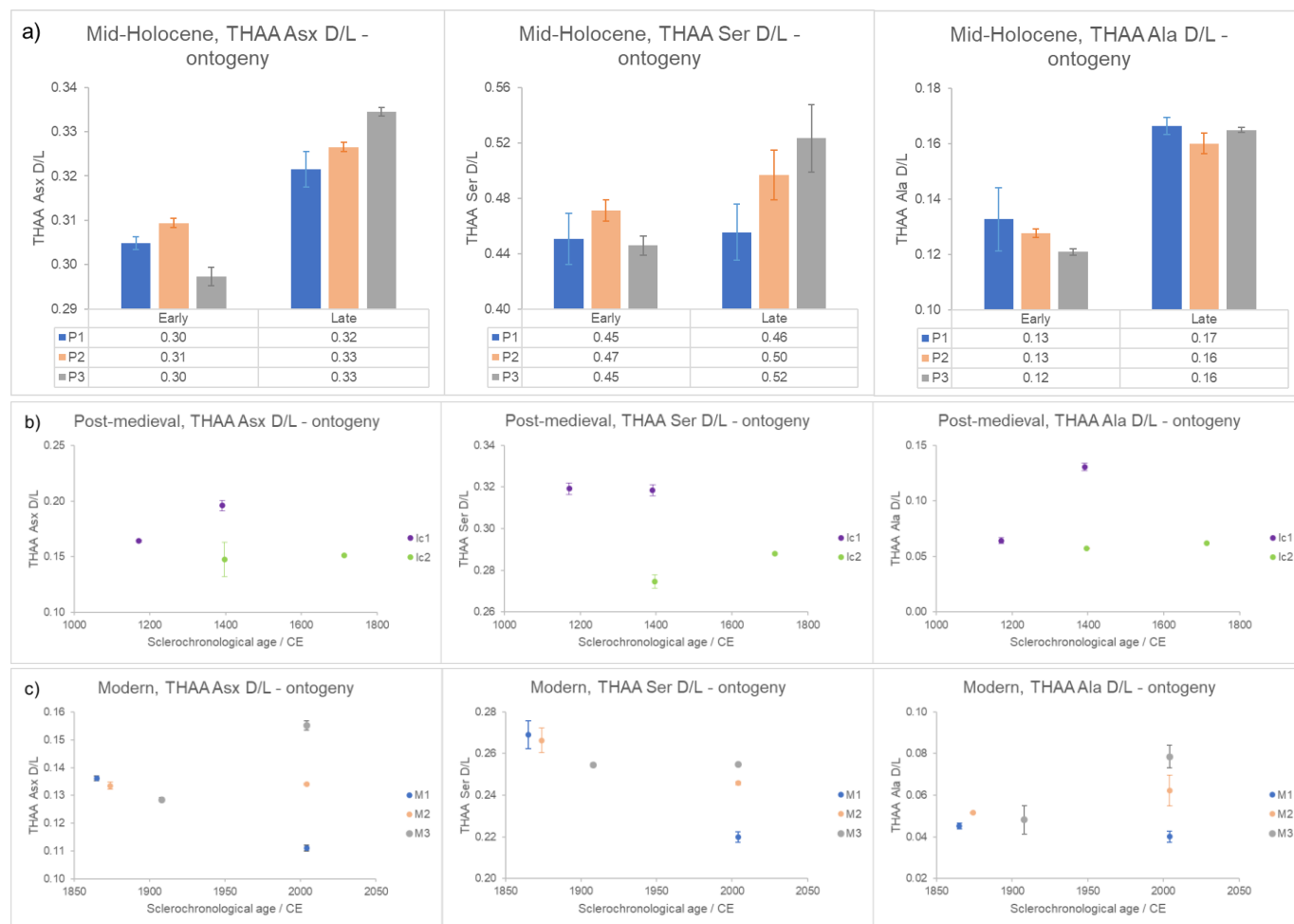
406 It is expected that the iOSL of samples from early ontogeny will have higher D/L values, because this part of the biomineral
407 would have been deposited earlier in time; late ontogenetic samples will have lower D/L values. As the fastest racemising
408 amino acids (Fig. 9a; Supplementary information Fig. S3), Asx, Ser and Ala were examined in detail (Fig. 11). The error bars
409 are quite large in the FAA samples, likely due to the low concentrations of amino acids, so the data should be treated with



410 caution and therefore only the THAA are going to be discussed here. In the Mid-Holocene samples the D/L values for Asx,
411 Ser and Ala show higher values in late ontogeny, contrary to the expectation (Fig. 11a). The intra-shell variability is very low
412 ($\sigma=0.005-0.02$ for FAA and THAA), and the lack of ontogenetic trend is likely related to the older age of the shells confounding
413 the *in vivo* degradation. The post-medieval shells do not show any significant ontogenetic pattern (Fig. 11b). The expected
414 higher D/L values in early ontogeny are present in the modern shells FAA Asx, THAA Asx and Ser D/L plots, but not for Ala
415 (Fig. 11c). Similarly to our data, Goodfriend and Weidman (2001) showed a gradual decrease in D/L in the unbleached outer
416 layer of modern *A. islandica* shells from the umbo to the rim, but the trend was less evident in subfossil shells, especially in
417 increments older than 1050 ± 35 (^{14}C age). The increments in early ontogeny also showed a much higher extent of racemisation
418 connected with fast growth and large band ages compared to the rest of the shell, indicating that there are different proteins
419 responsible for shell growth in early and late ontogeny (Goodfriend and Weidman, 2001). As a result, they recommended
420 consistent sampling of the iOSL layer in late ontogeny or at least after increment year 20 (Goodfriend and Weidman, 2001).

421 It is notable that the D/L values in the THAA fraction of modern samples in early ontogeny follow the year of birth in the
422 THAA fraction (Fig. 11c): meaning that the eldest shell that settled from larva first in 1865 has highest D/L (Fig. 11b, M1,
423 blue circle), followed by the shell represented by the orange circle (Fig. 11b, M2) settled in 1874 and the least racemised
424 sample is the shell that was settled in 1908 (Fig. 11b, M3, grey circle). For the post-medieval shells, intra-shell variation is
425 high, especially for the D/L values corresponding to ~ 1400 CE. Similarly, the late ontogeny modern shells (Fig. 11c, M1,
426 M2, M3) all died in 2004 and should have similar D/L values, but they show great variability and/or large error bars, except
427 for the FAA Asx D/L values.

428 The concentration of amino acids is higher in early ontogeny samples in the Md-Holocene shells from the North Sea,
429 whereas the opposite trend is observed in the post-medieval and modern shells (Supplementary information Fig. S6).
430 Goodfriend and Weidman (2001) observed a slight decrease in percentage composition of Ser, Tyr, Met, Ile and Leu with
431 age and an increase in Glu, Val, Ala and Asp with age. Overall, there is no specific trend in composition with ontogeny in
432 our shells, although some of the palaeontological and modern shells show similar results to Goodfriend and Weidman
433 (2001), indicating that there may be more acidic intra-crystalline proteins responsible for growth during early ontogeny
434 compared to late ontogeny, where basic amino acids are more prominent (Supplementary information, Fig. S6). The
435 different proteins in early and late ontogeny may also be responsible for the variability in D/L. In summary, the D/L values
436 in early and late ontogeny of modern, post-medieval and Mid-Holocene age have high intra-shell and inter-shell variability,
437 suggesting that AAG is not suitable for providing *within*-shell chronologies in *A. islandica* shells. Given the possible
438 variability in D/L values and protein composition with ontogeny, it is recommended to consistently sample the iOSL layer
439 for AAG; late ontogeny is preferred because of the increased thickness of the iOSL layer.



440

441

442

443 Figure 11. THAA Asx, Ser and Ala D/L for (a) Mid-Holocene, (b) post-medieval, (c) modern *A. islandica* early and late
 444 ontogeny samples. Note: the age sampled for AAG may vary slightly from the sclerochronological age reported. Error bars
 445 indicate one standard deviation based on two analytical replicates. Except for the modern samples, AAG shows no ontogenetic
 446 trends

447 **3.5 Optimised method and recommendations**

448 The bleaching experiments have shown that the IcP of all three microstructural layers can be isolated after 48 h of bleaching
 449 (Figs. 4-5; Sec. 3.2). Heating experiments showed that all layers behave as a closed system. The ISL has a higher rate of
 450 peptide bond hydrolysis (Fig. 8), likely due to the higher percentage composition of labile amino acids compared to the outer
 451 layers. The slightly higher scattering in D/L values in the ISL (Fig. 9b) suggests the use of the outer shell layer for future



452 dating. The low peptide bond hydrolysis and co-variance between FAA and THAA in the oOSL and iOSL suggests that these
453 layers may provide more reliable dating (Sec. 3.3). Given that the iOSL is easier for sampling, as this layer is the widest, and
454 is already used in sclerochronological and isotope studies, we recommend using this layer for AAG. From the ontogenetic
455 trends observed (Sec. 3.4), it is recommended to sample the late ontogeny (near the margin) portion of the iOSL; this should
456 ensure more consistent protein analysis.

457 In conclusion, for AAG analysis of *A. islandica* we recommend cleaning of the shell in deionised water with sonication and
458 selective drilling of the iOSL from a portion deposited in late ontogeny. The drilling step can be done by slicing the shell from
459 the umbo to the margin (Sec. 2.2), and then either selectively drilling the iOSL with a hand-held rotary burr if this layer is
460 thick, or drilling the oOSL away until the iOSL is reached and collecting only the latter layer. Caution needs to be taken to
461 continuously move the rotary burr to reduce the build-up of temperature that can degrade the protein (Sec. 3.1). The powdered
462 iOSL is then exposed to NaOCl for 48h and removed by washing with water and MeOH. The demineralisation, hydrolysis
463 and UHPLC analysis steps are outlined in section 2.

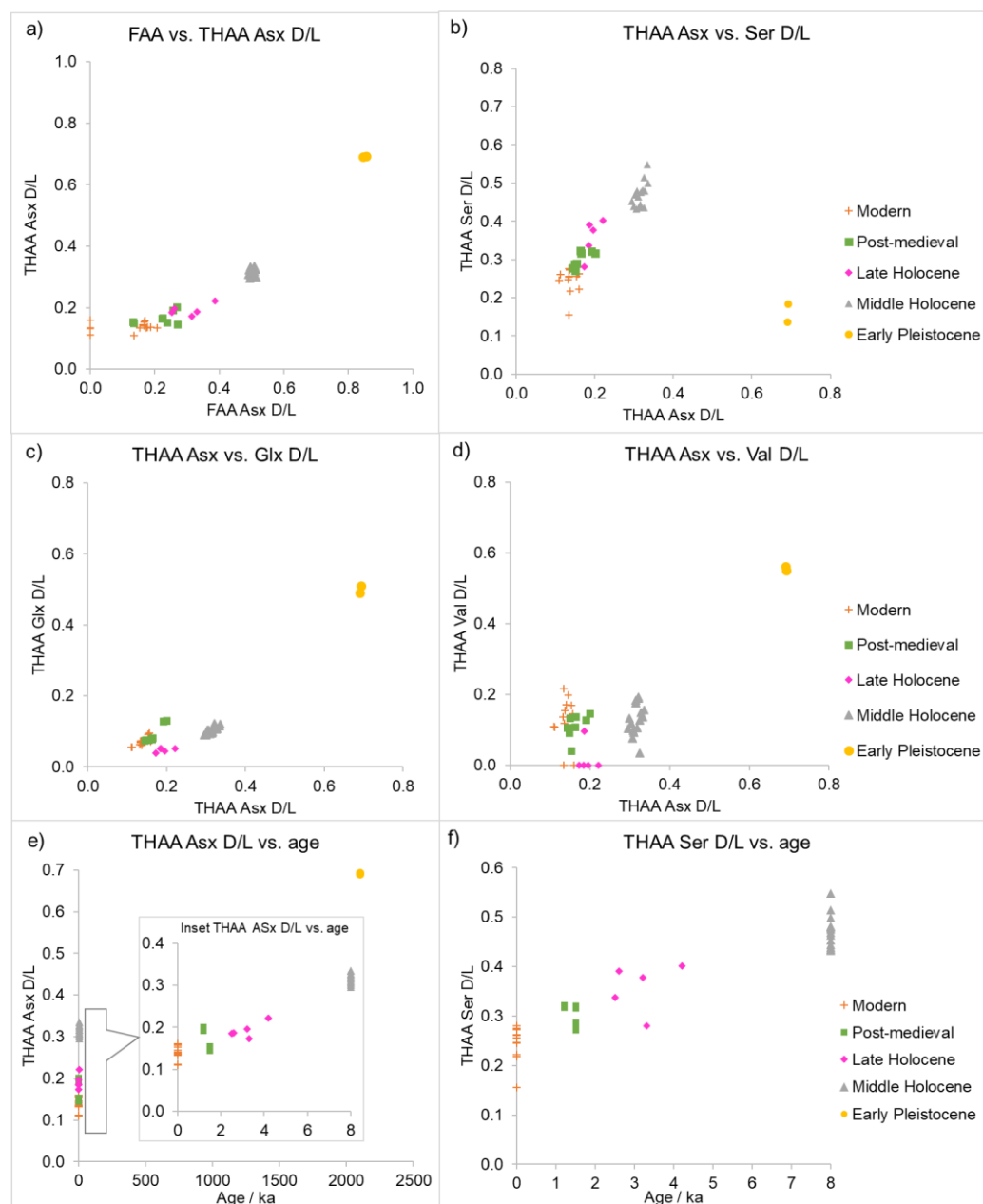
464 **3.6 An initial IcpD AAG framework for *A. islandica***

465 Following the isolation of a stable intra-crystalline protein fraction that shows effectively closed-system behaviour in the iOSL
466 of *A. islandica* in laboratory experiments, we analysed subfossil shells with independent evidence of age to observe the amino
467 acids' degradation patterns in *A. islandica* during the Quaternary period. The Quaternary shell samples used in this initial
468 framework were *A. islandica* already dated by sclerochronology, radiocarbon dating, subfossil evidence and AAG of other
469 material in the same horizon (Table 1; Butler et al., 2009, 2013; Estrella-Martinez, 2019; Preece et al., 2020; Supplementary
470 information Table S2). The iOSL was sampled, when possible, from late ontogeny for consistency of results. Samples were
471 prepared as outlined in sections 2 and 3.5.

472 In a closed-system the FAA and THAA D/L values are highly correlated and indicate that both fractions of amino acids degrade
473 predictably. From the high temperature experiments (Sec. 3.3) Asx and Ser were the fastest racemisers, meaning that they
474 should provide higher temporal resolution for dating more recent specimens. Glx, Val and Phe show slower racemisation
475 (Supplementary information, Fig. S3), thus they may be able to date earlier in the Quaternary period. In our subfossil samples
476 the FAA and THAA D/L show a high co-variance for Asx, and good correlation of THAA Glx, Ser and Asx (Fig. 12),
477 indicating that subfossil samples follow a predictable degradation pattern. In some amino acid parameters there seems to be
478 different degradation patterns when comparing the high temperature experiments and subfossils (Supplementary information
479 Fig. S7). This has been seen before in other biominerals (e.g. Tomiak et al., 2013; Dickinson et al., 2019; Baldreki et al.,
480 2024), and may be due either to limitations of these high temperature experiments, or different degradation pathways which
481 are enabled under high temperature conditions. Both preclude using this high temperature dataset to calculate kinetic



482 parameters for this biomineral. While the IcP framework is richer in the Holocene period and very limited for the Pleistocene,
483 the Early Pleistocene and Mid-Holocene samples are well-separated for all amino acids presented here, showing that it is
484 possible to distinguish between Pleistocene and Holocene samples using *A. islandica* (Fig. 12). However, using Glx and Val
485 (Figs. 12a, c, d) it is not possible to distinguish the modern and post-medieval shells. In the Asx and Ser plot (Fig. 12b) the
486 modern, post-medieval and Late Holocene (Walker et al., 2019) shells are better separated, although some overlap is still
487 present. In this plot, the THAA Ser values for the Early Pleistocene shells are lower than in modern shells, because free Ser
488 naturally decomposes with age as previously shown in the heating experiments (Sec. 3.3) and in other biominerals (Penkman
489 et al., 2008; Penkman, 2010; Crisp et al., 2013; Demarchi et al., 2013, 2015).



490

491 Figure 12. a) FAA vs. THAA Asx D/L; b) THAA Asx vs. Ser D/L; c) THAA Asx vs. Glx D/L; d) THAA Asx vs. Val D/L; e)
492 THAA Asx D/L vs. age and inset focusing on the last 8 ka; f) THAA Ser D/L vs. age of modern, post-medieval, Late Holocene,
493 Middle Holocene and Early Pleistocene *A. islandica* shells. D/L values for the slower racemising amino acids (e.g. Glx) span
494 the Quaternary period, while the faster racemising amino acids (e.g. Asx, Ser) allow temporal resolution within the Holocene.



495 These preliminary results indicate that it is possible to use the IcP in the iOSL of *A. islandica* for AAG of Quaternary shells.
496 The Early Pleistocene shells have very high D/Ls for the fast racemiser Asx in (FAA Asx D/L ~0.85; THAA Asx D/L ~0.69),
497 approaching the end-point for using Asx in AAG (Torres et al., 2013; Demarchi et al., 2013). Glx and Val D/L values were
498 lower (FAA Glx D/L ~0.63, Val D/L ~0.75; THAA Glx D/L ~0.50, Val D/L ~0.56) meaning that there is potential to use these
499 slower racemisers to date shells further back into the Pleistocene and Late Pliocene (Fig. 12c, d; Penkman et al., 2007; Reichert
500 et al., 2011; Hendy et al., 2012; Torres et al., 2013; Demarchi et al., 2013; Millman et al., 2022). On the Holocene timescale,
501 the fast racemisers Asx and Ser provide reliable D/L separation between the Middle and Late Holocene (Fig. 12f). Modern
502 samples have a slight overlap with post-medieval shells in THAA Ser and Asx, meaning that the resolution of AAG for *A.*
503 *islandica* for these amino acids may be approx. 1500-2000 years during the Middle and Late Holocene in the temperate-cold
504 climate of the North Sea. Given the non-linear nature of AAG, the resolution will be reduced into the Pleistocene, but further
505 analyses are required to assess the resolution. If samples date from the last ~50 ka, then radiocarbon dating will provide a
506 higher resolution dating method compared to AAG in the temperate-cold environment where *A. islandica* typically lives,
507 although it requires correction for the marine reservoir effect (Hajdas et al., 2021). Nevertheless, AAG using the IcP of the
508 iOSL of *A. islandica* has the potential to discriminate Middle and Late Holocene samples, and further back into the Early
509 Pleistocene or Late Pliocene.

510 **3.7 AAG rangefinding of undated shells**

511 Since the Middle and Late Holocene, important cultural transitions and palaeoenvironmental and ecological changes, both
512 natural and human-induced, have taken place in the North Sea and Iceland and had an impact on the marine ecosystem (for
513 example the Mesolithic-Neolithic transition, the settlements of Vikings in Iceland, and the Industrial Revolution in Northern
514 Europe (Andersen, 2000; Ahronson, 2012; Poulsen, 2008). The palaeoenvironmental record contained within subfossil *A.*
515 *islandica* provides a unique way to study these important transitions, but dating is required to identify potentially relevant
516 shells. As part of the ERC SEACHANGE project, over twenty thousand *A. islandica* shells were collected from the North Sea
517 and Iceland seafloors during research cruise DY150 in 2022, with the aim to use these for geochemical and sclerochronological
518 studies (Scourse et al., 2022). Here we explore the potential for rangefinding age estimates of individual dead shells by AAG.
519 The initial IcPD AAG framework showed the potential to provide dating of shells with resolution of 1500-2000 years during
520 the Middle and Late Holocene. The rangefinding is expected to narrow down the age of the shells collected from the North
521 Sea and Iceland seafloors (Supplementary information Table S2).

522 The AAG age range finding was carried out on 160 shells (Fig. 13; Supplementary information Table S2). The AAG dating
523 determined that these shells likely span the Middle and Late Holocene, with both the Asx and Ser D/L values in agreement
524 with this time period. In cases where there was agreement between the three most useful parameters for the Holocene (FAA



525 Asx D/L, THAA Asx D/L, and THAA Ser D/L), the narrowest age range possible was assigned (Fig. 13). It is noted that there
526 are a few shells that overlap between age periods, likely due to the resolution of AAG. In case of agreement of two of the
527 three D/L values, a wider age range was assigned. For example, shell Ic22200193 showed correlation with Late Holocene for
528 the THAA Asx and Ser D/L, but the FAA Asx D/L value overlapped between the Late Holocene and post-medieval age; due
529 to the agreement of two of the three parameters with the Late Holocene (which includes post-medieval), this shell was assigned
530 an age range correlating with this stage. Shell FG22202523 showed THAA Asx D/L indicating a modern age, but FAA Asx
531 D/L and THAA Ser D/L overlap between modern and post-medieval age, thus a post-medieval-modern age range was assigned.
532 These three screening methods resulted in 93 shells with a narrower age range and 67 shells with a wider age range (either
533 because of agreement of two of the three D/L, or overlap of D/L values between age ranges). There were four shells,
534 Ic22201300, Ic2220035, Ic22200194, Ic22202048, which showed D/L values consistently higher than the Late Holocene shells
535 but lower than the Mid-Holocene shells; thus, they were categorised as older than ~4 ka and younger than ~8 ka in age (8
536 ka < shells > 4 ka). Ten shells from the Fladen Ground exhibited THAA Asx and Ser D/L values slightly higher than the Mid-
537 Holocene D/L values, thus they were categorised as Early Holocene or older. The results of AAG rangefinding of *A. islandica*
538 shows that this technique is able to narrow down the ages of shells, assigning 10 shells to the Early Holocene or older, seven
539 shells as younger than ~8 ka and older than ~4 ka (8 ka < shells > 4 ka), 23 shells to the Late Holocene, 34 shells to post-medieval
540 age, and 86 modern shells. These analyses provide an initial age range for *A. islandica* shells that, depending on the time
541 period of interest, can then enable selection of appropriate shells for more accurate dating with radiocarbon,
542 sclerochronological crossdating and studied for palaeoecological information.

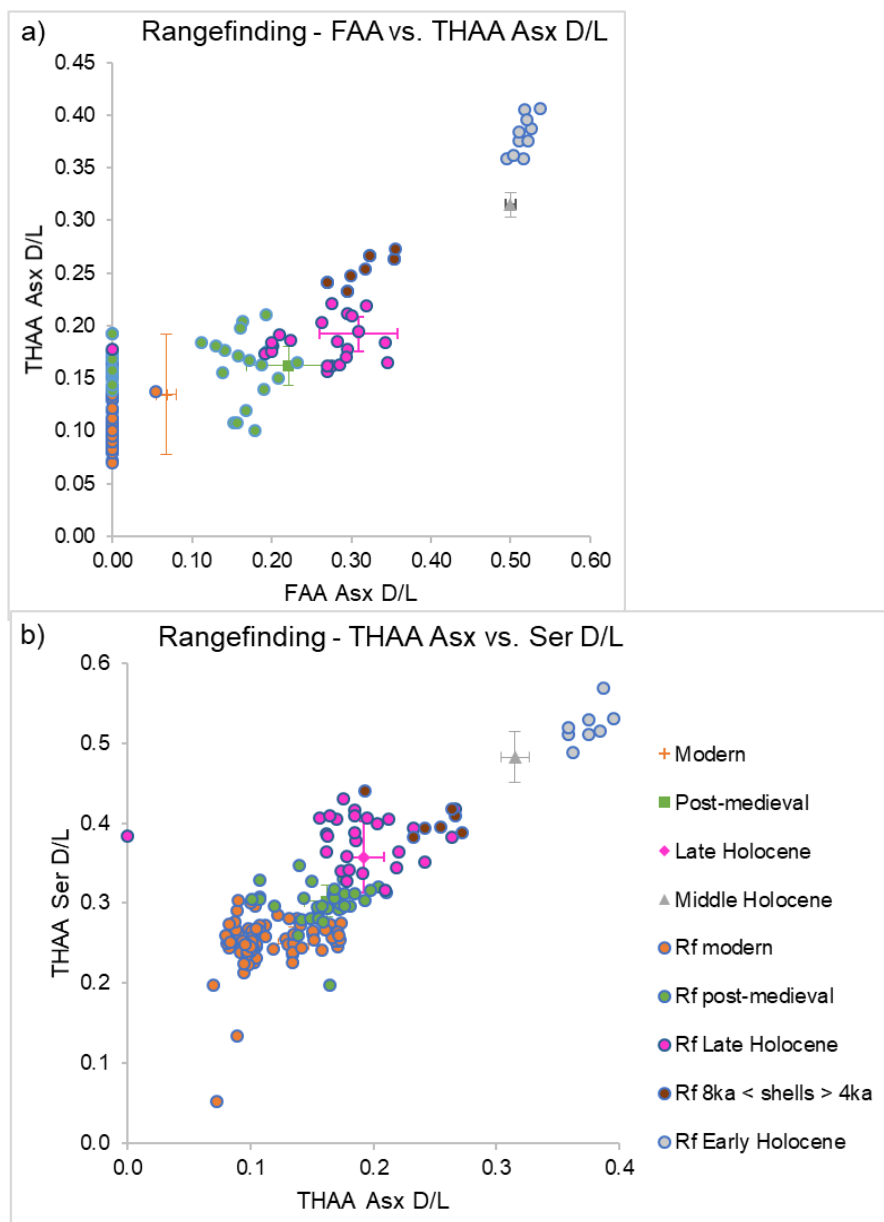


Figure 13. Rangefinding (Rf) of *A. islandica* shells within the IcPD framework (a) FAA vs. THAA Asx D/L, (b) THAA Asx vs. Ser D/L. Modern samples are in orange, post-medieval in green, Late Holocene shells in pink, shells older than ~4 ka and younger than ~8 ka (8 ka < shells > 4 ka) in brown, and Early Holocene in grey.



548 **4 Conclusion**

549 A protocol for the analysis of intra-crystalline chiral amino acids for amino acid geochronology (AAG) of the bivalve *A.*
550 *islandica* has been established. The three-layer microstructure of the shell has been investigated to determine which layer
551 would be most applicable to AAG. The intra-crystalline protein (IcP) fraction was successfully isolated with NaOCl oxidation
552 for 48 h. This analysis highlighted different amino acid compositions between the three layers (oOSL, iOSL and ISL), meaning
553 that for reliable dating a single microstructural layer should be sampled. Heating experiments at 140°C showed that the protein
554 fraction in the inner layer ISL is more prone to peptide bond hydrolysis than the outer layers, possible due to the high
555 composition of labile amino acids in this layer. Conversely, the outer layers show low loss and decomposition of amino acids.
556 Nevertheless, all three layers show good co-variance between FAA and THAA D/L and behave as a closed system. The iOSL
557 layer is recommended for AAG because it is already used for isotopic and sclerochronological studies. The oOSL, the
558 outermost layer, is more exposed to the external environment and marine organisms and is thinner than the iOSL, thus harder
559 to select. Samples of early and late ontogeny in modern, post-medieval and Mid-Holocene shells did not show a consistent
560 pattern of composition and D/L, thus the resolution and sensitivity of AAG is too low for sclerochronological studies *within*
561 *A. islandica* shells of this age. The optimised method of analysis of the iOSL, following bleaching for 48 h, was applied to
562 Quaternary subfossils, providing an initial dating framework, with the fast racemisers Asx and Ser able to distinguish Mid-
563 Holocene from post-medieval/modern samples, providing a tentative resolution for AAG of *A. islandica* of approx. 1500 years
564 in the Late Holocene. The slower racemising amino acids are able to date back to at least the Early Pleistocene. Ranging
565 of 160 undated shells showed that AAG can securely separate between modern, post-medieval (~1100-1700 CE), Late
566 Holocene (4-1 ka), Mid-Holocene (~8 ka) and Early Holocene (>8 ka) shells. Further analyses are required to expand the
567 framework and better establish the age resolution for this biomineral, but these initial promising results indicate that *A.*
568 *islandica* is a reliable biomineral for AAG dating of marine deposits during the Quaternary period and for ranging
569 collections of *A. islandica* shells of unknown age.

570 **Author contribution**

571 Conceptualisation: Kirsty E. H. Penkman, James D. Scourse

572 Data curation: Martina L. G. Conti

573 Formal analysis: Martina L. G. Conti, Kirsty E. H. Penkman

574 Funding acquisition: Kirsty E. H. Penkman, James D. Scourse

575 Investigation: Martina L. G. Conti, Kirsty E. H. Penkman

576 Methodology: Martina L. G. Conti, Kirsty E. H. Penkman



577 Project administration & supervision: Kirsty E.H. Penkman, James D. Scourse
578 Resources: Kirsty E. H. Penkman, Martina L. G. Conti, Paul G. Butler, David J. Reynolds, Tamara Trofimova, James D.
579 Scourse
580 Validation: Martina L. G. Conti, Paul G. Butler, David J. Reynolds, Tamara Trofimova, James D. Scourse, Kirsty E. H.
581 Penkman
582 Visualisation: Martina L. G. Conti, Kirsty E. H. Penkman
583 Writing - original draft preparation: Martina L. G. Conti, Kirsty E. H. Penkman
584 Writing - review and editing: Martina L. G. Conti, Kirsty E. H. Penkman, Paul G. Butler, David J. Reynolds, Tamara
585 Trofimova, James D. Scourse

586 **Competing interests**

587 Kirsty E. H. Penkman is an associate editor of the journal.

588 **Acknowledgments**

589 The authors declare that they have no conflict of interest.

590 The SEACHANGE Synergy Project has received funding from the European Research Council (ERC) under the European
591 Union's Horizon 2020 research and innovation programme (Grant Agreement No 856488).

592 Iceland radiocarbon dates were funded by the EU Framework 6 MILLENNIUM Integrated Project 'European climate of the
593 last millennium' (SUSTDEV-2004-3.1.4.1, 017008-2).

594 North Sea radiocarbon dates were funded by European Union Fifth Framework HOLSMEER project (EVK2-CT-2000-00060)
595 and the United Kingdom Natural Environment Research Council standard research grant (NER/A/S/2002/00809)

596 Thanks to Mr. J. Scolding, Dr. Anna Genelt-Yanovskaya and Dr. R. Preece for providing some of the samples. Thanks to Dr.
597 Niklas Hausmann for discussing initial sampling techniques and for providing samples. Dr S. Presslee and Mr. M. von Tersch
598 are thanked for initial laboratory training and Ms. S. Taylor for administrative support. Many thanks to Dr. Lucy Wheeler, Dr.
599 Marc Dickinson & Ms. C. Båldreki for helpful comments on an initial version of this manuscript.



600 **Open access policy**

601 For the purpose of open access, the author has applied a Creative Commons Attribution (CC BY) licence to any Author
602 Accepted Manuscript version arising from this submission.

603 **Data availability**

604 Data in this study has been included in the Supplementary information Table S2 and all amino acid data from this study will
605 be made available through the NOAA repository upon publication: <ftp://ftp.ncdc.noaa.gov/pub/data/paleo/aar/>.

606 **References**

- 607 Abelson, P.H. (1955) Organic constituents of fossils. *Carnegie Institute of Washington Year Book*, 54, 107-9
- 608 Ahronson, K. (2012) Seljaland: archaeology, palaeoecology and tephrochronology. In Larsen G, Eiriksson J (eds.) *Holocene*
609 *Tephrochronology. Applications in South Iceland*. Field Guide. *Quaternary Research Association*, London. pp 61-66.
- 610 Alves, E. Q., Macario, K., Ascough, P. & Bronk Ramsey, C. (2018). The worldwide marine radiocarbon reservoir effect:
611 Definitions, mechanisms, and prospects. *Reviews of Geophysics*, 56, 278–305. <https://doi.org/10.1002/2017RG000588>
- 612 Andersen, SH 2000. ‘Køkkenmøddinger’ (shell middens) in Denmark: A survey. proceedings of the Prehistoric Society 66,
613 361–84.
- 614 Bada, J. L. (1972). Kinetics of Racemization of Amino Acids as a Function of pH. *Journal of the American Chemical Society*,
615 94(4), 1371–1373.
- 616 Bada, J. L., Shou, M. Y., Man, E. H., & Schroeder, R. A. (1978). Decomposition of hydroxy amino acids in foraminiferal tests;
617 kinetics, mechanism and geochronological implications. *Earth and Planetary Science Letters*, 41(1), 67–76.
618 [https://doi.org/10.1016/0012-821X\(78\)90042-0](https://doi.org/10.1016/0012-821X(78)90042-0)
- 619 Baldreki, C., Burnham, A., Conti, M., Wheeler, L., Simms, M. J., Barham, L., White, T. S., & Penkman, K. (2024).
620 Investigating the potential of African land snail shells (Gastropoda: Achatininae) for amino acid geochronology. *Quaternary*
621 *Geochronology*, 79. <https://doi.org/10.1016/j.quageo.2023.101473>



- 622 Baleka, S., Herridge, V. L., Catalano, G., Lister, A. M., Dickinson, M. R., di Patti, C., Barlow, A., Penkman, K. E. H., Hofreiter,
623 M., & Pajmans, J. L. A. (2021). Estimating the dwarfing rate of an extinct Sicilian elephant. *Current Biology*, 31(16), 3606-
624 3612.e7. <https://doi.org/10.1016/j.cub.2021.05.037>
- 625 Bhattacharyya, S. K., & Banerjee, A. B. (1974). D-Amino Acids in the Cell Pool of Bacteria. *Folia Microbiol*, 19, 43–50.
- 626 Brand U, Morrison JO. Paleocene #6. Biogeochemistry of fossil marine invertebrates. *Geoscience Canada*. 1987
627 Jun;14(2):85-107.
- 628 Bridgland, D. R., Harding, P., Allen, P., Candy, I., Cherry, C., George, W., Horne, D. J., Keen, D. H., Penkman, K. E. H.,
629 Preece, R. C., Rhodes, E. J., Scaife, R., Schreve, D. C., Schwenninger, J.-L., Slipper, I., Ward, G. R., White, M. J., White, T.
630 S., & Whittaker, J. E. (2013). An enhanced record of MIS 9 environments, geochronology and geoarchaeology: data from
631 construction of the High Speed 1 (London–Channel Tunnel) rail-link and other recent investigations at Purfleet, Essex, UK.
632 *Proceedings of the Geologists' Association*, 124(3), 417–476. <https://doi.org/10.1016/j.pgeola.2012.03.006>
- 633 Bright, J., & Kaufman, D. S. (2011). Amino acids in lacustrine ostracodes, part III: Effects of pH and taxonomy on
634 racemization and leaching. *Quaternary Geochronology*, 6(6), 574–597. <https://doi.org/10.1016/j.quageo.2011.08.002>
- 635 Brooks, A. S., Hare, P. E., Kokis, J. E., Miller, G. H., Ernst, R. D., & Wendorf, F. (1990). Dating Pleistocene Archeological
636 Sites by Protein Diagenesis in Ostrich Eggshell. *Science*, 248(4951), 60–64. <https://www.science.org>
- 637 Brosset, C., Höche, N., Shirai, K., Nishida, K., Mertz-Kraus, R., & Schöne, B. R. (2022). Strong Coupling between Biomineral
638 Morphology and Sr/Ca of *Arctica islandica* (Bivalvia)—Implications for Shell Sr/Ca-Based Temperature Estimates. *Minerals*,
639 12(5). <https://doi.org/10.3390/min12050500>
- 640 Butler, P. G., Richardson, C. A., Scourse, J. D., Witbaard, R., Schöne, B. R., Fraser, N. M., Wanamaker, A. D., Bryant, C. L.,
641 Harris, I., & Robertson, I. (2009). Accurate increment identification and the spatial extent of the common signal in five *Arctica*
642 *islandica* chronologies from the Fladen Ground, northern North Sea. *Paleoceanography*, 24(2).
643 <https://doi.org/10.1029/2008PA001715>
- 644 Butler, P. G., Wanamaker, A. D., Scourse, J. D., Richardson, C. A., & Reynolds, D. J. (2013). Variability of marine climate
645 on the North Icelandic Shelf in a 1357-year proxy archive based on growth increments in the bivalve *Arctica islandica*.
646 *Palaeogeography, Palaeoclimatology, Palaeoecology*, 373, 141–151. <https://doi.org/10.1016/j.palaeo.2012.01.016>
- 647 Crippa, G., Azzarone, M., Bottini, C., Crespi, S., Felletti, F., Marini, M., Petrizzo, M. R., Scarponi, D., Raffi, S., & Raineri,
648 G. (2019). Bio-and lithostratigraphy of lower Pleistocene marine successions in western Emilia (Italy) and their implications



- 649 for the first occurrence of *Arctica islandica* in the Mediterranean Sea. *Quaternary Research (United States)*, 92(2), 549–569.
650 <https://doi.org/10.1017/qua.2019.20>
- 651 Crisp, M. K. (2013). Amino acid racemization dating: Method development using African ostrich (*Struthio camelus*) eggshell.
652 PhD thesis, University of York.
- 653 Crisp, M., Demarchi, B., Collins, M., Morgan-Williams, M., Pilgrim, E., & Penkman, K. (2013). Isolation of the intra-
654 crystalline proteins and kinetic studies in *Struthio camelus* (ostrich) eggshell for amino acid geochronology. *Quaternary*
655 *Geochronology*, 16, 110–128. <https://doi.org/10.1016/j.quageo.2012.09.002>
- 656 Davies, B. J., Bridgland, D. R., Roberts, D. H., Cofaigh, C. Ó., Pawley, S. M., Candy, I., Demarchi, B. (2009). The age and
657 stratigraphic context of the Easington Raised Beach, County Durham, UK. *Proceedings of the Geologists' Association*, 120,
658 4, 183-198.
- 659 Demarchi, B., Clements, E., Coltorti, M., van de Locht, R., Kröger, R., Penkman, K., & Rose, J. (2015). Testing the effect of
660 bleaching on the bivalve *Glycymeris*: A case study of amino acid geochronology on key Mediterranean raised beach deposits.
661 *Quaternary Geochronology*, 25, 49–65. <https://doi.org/10.1016/j.quageo.2014.09.003>
- 662 Demarchi, B., Collins, M. J., Tomiak, P. J., Davies, B. J., & Penkman, K. E. H. (2013b). Intra-crystalline protein diagenesis
663 (IcPD) in *Patella vulgata*. Part II: Breakdown and temperature sensitivity. *Quaternary Geochronology*, 16, 158–172.
664 <https://doi.org/10.1016/j.quageo.2012.08.001>
- 665 Demarchi, B. Geochronology of coastal prehistoric environments: a new closed system approach using amino acid
666 racemisation. PhD thesis, University of York.
- 667 Demarchi, B., Rogers, K., Fa, D. A., Finlayson, C. J., Milner, N., & Penkman, K. E. H. (2013a). Intra-crystalline protein
668 diagenesis (IcPD) in *Patella vulgata*. Part I: Isolation and testing of the closed system. *Quaternary Geochronology*, 16, 144–
669 157. <https://doi.org/10.1016/j.quageo.2012.03.016>
- 670 Dickinson, M. R., Lister, A. M., & Penkman, K. E. H. (2019). A new method for enamel amino acid racemization dating: A
671 closed system approach. *Quaternary Geochronology*, 50, 29–46. <https://doi.org/10.1016/j.quageo.2018.11.005>
- 672 Dominguez, J. G., Kosnik, M. A., Allen, A. P., Hua, Q., Jacob, D. E., Kaufman, D. S., & Whitacre, K. (2016). Time-averaging
673 and stratigraphic resolution in death assemblages and Holocene deposits. *Source: PALAIOS*, 31(11), 564–575.
674 <https://doi.org/10.2307/26780062>



- 675 Dunca, E., Mutvei, H., Göransson, P., Mörth, C. M., Schöne, B. R., Whitehouse, M. J., Elfman, M., & Baden, S. P. (2009).
676 Using ocean quahog (*Arctica islandica*) shells to reconstruct palaeoenvironment in Öresund, Kattegat and Skagerrak, Sweden.
677 *International Journal of Earth Sciences*, 98(1), 3–17. <https://doi.org/10.1007/s00531-008-0348-6>
- 678 Estrella-Martínez, J., Ascough, P. L., Schöne, B. R., Scourse, J. D., & Butler, P. G. (2019). 8.2 ka event North Sea hydrography
679 determined by bivalve shell stable isotope geochemistry. *Scientific Reports*, 9(1), 1–9. [https://doi.org/10.1038/s41598-019-](https://doi.org/10.1038/s41598-019-43219-1)
680 43219-1
- 681 Estrella-Martínez, J. (2019). Holocene climate variability in UK waters based on *Arctica islandica* sclerochronology. PhD
682 thesis, Bangor University.
- 683 Eyles, N., McCabe, A. M., & Bowen, D. Q. (1994). The stratigraphic and sedimentological significance of Late Devensian Ice
684 Sheet surging in Holderness, Yorkshire, U.K. *Quaternary Science Reviews*, 13(8), 727–759. [https://doi.org/10.1016/0277-](https://doi.org/10.1016/0277-3791(94)90102-3)
685 3791(94)90102-3
- 686 Goodfriend, G. A., Hare, P. E., & Druffel, E. R. M. (1992). Aspartic acid racemization and protein diagenesis in corals over
687 the last 350 years. In *Geochimica et Cosmochimica Acta* (Vol. 56, pp. 3847–3850). [https://doi.org/10.1016/0016-](https://doi.org/10.1016/0016-7037(94)00324-F)
688 7037(94)00324-F
- 689 Goodfriend, G. A., & Weidman, C. R. (2001). Ontogenetic trends in aspartic acid racemization and amino acid composition
690 within modern and fossil shells of the bivalve *Arctica*. *Geochimica et Cosmochimica Acta*, 65(12), 1921–1932.
691 [https://doi.org/10.1016/S0016-7037\(01\)00564-6](https://doi.org/10.1016/S0016-7037(01)00564-6)
- 692 Goodfriend, G. A., Flessa, K. W., & Hare, P. E. (1997). Variation in amino acid epimerization rates and amino acid
693 composition among shell layers in the bivalve *Chione* from the Gulf of California. *Geochimica et Cosmochimica Acta*, 61, 7,
694 1487-1493.
- 695 Goodfriend, G. A., Kashgarian, M., & Harasewych, M. G. (1995). Use of aspartic acid racemization and post-bomb ¹⁴C to
696 reconstruct growth rate and longevity of the deep-water slit shell *Entemnotrochus adansonianus*. *Geochimica et Cosmochimica*
697 *Acta*, 59(6), 1125–1129. <https://www.sciencedirect.com/science/article/pii/001670379500029Y>
- 698 Gries, K., Kröger, R., Kübel, C., Fritz, M., & Rosenauer, A. (2009). Investigations of voids in the aragonite platelets of nacre.
699 *Acta Biomaterialia*, 5(8), 3038–3044. <https://doi.org/10.1016/j.actbio.2009.04.017>
- 700 Hajdas, I., Ascough, P., Garnett, M. H., Fallon, S. J., Pearson, C. L., Quarta, G., Spalding, K. L., Yamaguchi, H., & Yoneda,
701 M. (2021). Radiocarbon dating. *Nature Reviews Methods Primers*, 1(1), 62. <https://doi.org/10.1038/s43586-021-00058-7>



- 702 Hare PE, Abelson PH. 1968. Racemization of amino acids in fossil shells. *Carnegie Institute of Washington Yearbook* 66:526-
703 8
- 704 Hare PE, Mitterer RM. 1969. Laboratory Simulation of amino acid diagenesis in fossils. *Carnegie Institute of Washington*
705 *Yearbook* 67:205-8
- 706 Haugen, J. E., & Sejrup, H. P. (1992). Isoleucine epimerization kinetics in the shell of *Arctica islandica*. *Norsk Geologisk*
707 *Tidsskrift*, 72(2), 171–180. https://foreninger.uio.no/ngf/ngt/pdfs/NGT_72_2_171-180.pdf
- 708 Haugen, J.-E., & Sejrup, H. P. (1990). Amino acid composition of aragonitic concholin in the shell of *Arctica islandica*.
709 *Lethaia*, 23(2), 133–141. <https://doi.org/10.1111/j.1502-3931.1990.tb01354.x>
- 710 Heaton, T. J., P. Köhler, M. Butzin, E. Bard, R. W. Reimer, W. E. N. Austin, C. Bronk Ramsey, P. M. Grootes, K. A. Hughen,
711 B. Kromer, P. J. Reimer, J. Adkins, A. Burke, M. S. Cook, J. Olsen, and L. C. Skinner. 2020: Marine20—The Marine
712 Radiocarbon Age Calibration Curve (0–55,000 cal BP). *Radiocarbon* 62:779–820. doi:10.1017/RDC.2020.68
- 713 Hendy, E. J., Tomiak, P. J., Collins, M. J., Hellstrom, J., Tudhope, A. W., Lough, J. M., & Penkman, K. E. H. (2012). Assessing
714 amino acid racemization variability in coral intra-crystalline protein for geochronological applications. *Geochimica et*
715 *Cosmochimica Acta*, 86, 338–353. <https://doi.org/10.1016/j.gca.2012.02.020>
- 716 Kaufman, D. S., & Manley, W. F. (1998). A new procedure for determining dl amino acid ratios in fossils using reverse phase
717 liquid chromatography. *Quaternary Science Reviews*, 17(11), 987–1000. [https://doi.org/10.1016/S0277-3791\(97\)00086-3](https://doi.org/10.1016/S0277-3791(97)00086-3)
- 718 Kosnik, M. A., & Kaufman, D. S. (2008). Identifying outliers and assessing the accuracy of amino acid racemization
719 measurements for geochronology: II. Data screening. *Quaternary Geochronology*, 3(4), 328–341.
720 <https://doi.org/10.1016/j.quageo.2008.04.001>
- 721 Kriausakul, N., & Mitterer, R. M. (1978). Isoleucine epimerization in peptides and proteins: kinetic factors and application to
722 fossil proteins. *Science (New York, N.Y.)*, 201(4360), 1011–1014. <https://doi.org/10.1126/science.201.4360.1011>
- 723 Malatesta, A., & Zarlenga, F. (1986). Northern guests in the Pleistocene Mediterranean sea. *Geologica Romana*, 25, 91–154.
- 724 Marchitto, T. M., Jones, G. A., Goodfriend, G. A., & Weidman, C. R. (2000). Precise Temporal Correlation of Holocene
725 Mollusk Shells Using Sclerochronology. *Quaternary Research*, 53(2), 236–246. <https://doi.org/10.1006/qres.1999.2107>



- 726 Milano, S., Nehrke, G., Wanamaker, A. D., Ballesta-Artero, I., Brey, T., & Schöne, B. R. (2017b). The effects of environment
727 on *Arctica islandica* shell formation and architecture. *Biogeosciences*, 14(6), 1577–1591. [https://doi.org/10.5194/bg-14-1577-](https://doi.org/10.5194/bg-14-1577-2017)
728 2017
- 729 Milano, S., Schöne, B. R., & Witbaard, R. (2017a). Changes of shell microstructural characteristics of *Cerastoderma edule*
730 (*Bivalvia*) — A novel proxy for water temperature. *Palaeogeography, Palaeoclimatology, Palaeoecology*, 465, 395–406.
731 <https://doi.org/10.1016/j.palaeo.2015.09.051>
- 732 Mitterer, R. M. (1975). Ages and diagenetic temperatures of pleistocene deposits of Florida based on isoleucine epimerization
733 in *Mercenaria*. *Earth and Planetary Science Letters*, 28(2), 275–282. [https://doi.org/10.1016/0012-821X\(75\)90237-X](https://doi.org/10.1016/0012-821X(75)90237-X)
- 734 Orem, C. A., & Kaufman, D. S. (2011). Effects of basic pH on amino acid racemization and leaching in freshwater mollusk
735 shell. *Quaternary Geochronology*, 6(2), 233–245. <https://doi.org/10.1016/j.quageo.2010.11.005>
- 736 Ortiz, J. E., Gutiérrez-Zugasti, I., Torres, T., González-Morales, M., & Sánchez-Palencia, Y. (2015). Protein diagenesis in
737 *Patella* shells: Implications for amino acid racemisation dating. *Quaternary Geochronology*, 27, 105–118.
738 <https://doi.org/10.1016/j.quageo.2015.02.008>
- 739 Ortiz, J. E., Sánchez-Palencia, Y., Gutiérrez-Zugasti, I., Torres, T., & González-Morales, M. (2018). Protein diagenesis in
740 archaeological gastropod shells and the suitability of this material for amino acid racemisation dating: *Phorcus lineatus* (da
741 Costa, 1778). *Quaternary Geochronology*, 46, 16–27. <https://doi.org/10.1016/j.quageo.2018.02.002>
- 742 Ortiz, J. E., Torres, T., & Pérez-González, A. (2013). Amino acid racemization in four species of ostracodes: Taxonomic,
743 environmental, and microstructural controls. *Quaternary Geochronology*, 16, 129–143.
744 <https://doi.org/10.1016/j.quageo.2012.11.004>
- 745 Ortiz, J. E., Torres, T., González-Morales, M. R., Abad, J., Arribas, I., Fortea, F. J., Garcia-Belenguer, F., & Gutiérrez-Zugasti,
746 I. (2009). The aminochronology of man-induced shell middens in caves in Northern Spain. *Archaeometry*, 51(1), 123–139.
747 <https://doi.org/10.1111/j.1475-4754.2008.00383.x>
- 748 Penkman, K. (2010). Amino acid geochronology: Its impact on our understanding of the Quaternary stratigraphy of the British
749 Isles. *Journal of Quaternary Science*, 25(4), 501–514. <https://doi.org/10.1002/jqs.1346>
- 750 Penkman, K. E. H., Preece, R. C., Keen, D. H., Maddy, D., Schreve, D. C., & Collins, M. J. (2007). Testing the
751 aminostratigraphy of fluvial archives: the evidence from intra-crystalline proteins within freshwater shells. *Quaternary Science*
752 *Reviews*, 26(22–24), 2958–2969. <https://doi.org/10.1016/j.quascirev.2007.06.034>



- 753 Penkman, K. E. H. H., Kaufman, D. S., Maddy, D., & Collins, M. J. (2008). Closed-system behaviour of the intra-crystalline
754 fraction of amino acids in mollusc shells. *Quaternary Geochronology*, 3(1–2), 2–25.
755 <https://doi.org/10.1016/j.quageo.2007.07.001>
- 756 Poulsen, B. (2008). Dutch Herring - An Environmental History, c. 1600-1860. Amsterdam University.
- 757 Preece, R. C., & Penkman, K. E. H. (2005). New faunal analyses and amino acid dating of the Lower Palaeolithic site at East
758 Farm, Barnham, Suffolk. *Proceedings of the Geologists' Association*, 116(3–4), 363–377. [https://doi.org/10.1016/S0016-7878\(05\)80053-7](https://doi.org/10.1016/S0016-7878(05)80053-7)
- 760 Preece, R. C., Meijer, T., Penkman, K. E. H., Demarchi, B., Mayhew, D. F., & Parfitt, S. A. (2020). The palaeontology and
761 dating of the 'Weybourne Crag', an important marker horizon in the Early Pleistocene of the southern North Sea basin.
762 *Quaternary Science Reviews*, 236. <https://doi.org/10.1016/j.quascirev.2020.106177>
- 763 Reynolds, D. J., Scourse, J. D., Halloran, P. R., Nederbragt, A. J., Wanamaker, A. D., Butler, P. G., Richardson, C. A.,
764 Heinemeier, J., Eiríksson, J., Knudsen, K. L., & Hall, I. R. (2016). Annually resolved North Atlantic marine climate over the
765 last millennium. *Nature Communications*, 7(2), 201–217. <https://doi.org/10.1038/ncomms13502>
- 766 Schöne, B. R., Freyre Castro, A. D., Fiebig, J., Houk, S. D., Oschmann, W., & Kröncke, I. (2004). Sea surface water
767 temperatures over the period 1884-1983 reconstructed from oxygen isotope ratios of a bivalve mollusk shell (*Arctica islandica*,
768 southern North Sea). *Palaeogeography, Palaeoclimatology, Palaeoecology*, 212(3–4), 215–232.
769 <https://doi.org/10.1016/j.palaeo.2004.05.024>
- 770 Schöne, B. R., & Fiebig, J. (2009). Seasonality in the North Sea during the Allerød and Late Medieval Climate Optimum using
771 bivalve sclerochronology. *International Journal of Earth Sciences*, 98(1), 83–98. <https://doi.org/10.1007/s00531-008-0363-7>
- 772 Schöne, B. R. (2013). *Arctica islandica* (Bivalvia): A unique paleoenvironmental archive of the northern North Atlantic Ocean.
773 *Global and Planetary Change*, 111, 199–225. <https://doi.org/10.1016/j.gloplacha.2013.09.013>
- 774 Schöne, B. R., & Huang, Q. (2021). Ontogenetic $\delta^{15}\text{N}$ Trends and Multidecadal Variability in Shells of the Bivalve Mollusk,
775 *Arctica islandica*. *Frontiers in Marine Science*, 8(748593), 1–15. <https://doi.org/10.3389/fmars.2021.748593>
- 776 Schöne, B. R., Dunca, E., Fiebig, J., & Pfeiffer, M. (2005b). Mutvei's solution: An ideal agent for resolving microgrowth
777 structures of biogenic carbonates. *Palaeogeography, Palaeoclimatology, Palaeoecology*, 228(1–2), 149–166.
778 <https://doi.org/10.1016/j.palaeo.2005.03.054>



- 779 Schöne, B. R., Fiebig, J., Pfeiffer, M., Gleß, R., Hickson, J., Johnson, A. L. A., Dreyer, W., & Oschmann, W. (2005a). Climate
780 records from a bivalved Methuselah (*Arctica islandica*, Mollusca; Iceland). *Palaeogeography, Palaeoclimatology,*
781 *Palaeoecology*, 228(1–2), 130–148. <https://doi.org/10.1016/j.palaeo.2005.03.049>
- 782 Scourse, J. D., Wanamaker, A. D., Weidman, C., Heinemeier, J., Reimer, P. J., Butler, P. G., Witbaard, R., & Richardson, C.
783 A. (2012): The marine radiocarbon bomb pulse across the temperate North Atlantic: A compilation of $\delta^{14}\text{C}$ time histories from
784 *Arctica islandica* growth increments. *Radiocarbon* 54:165–186. doi:10.2458/azu_js_rc.v54i2.16026
- 785 Scourse, J. D., Afrifa, K., Byrne, L., Crowley, D., Earland, J. L., Ehmen, T., Frøslev, T. G., Greenall, C., Harland, J., Heard,
786 Z., Höche, N., Holman, L. E., Huang, Q., Langkjær, E. M. R., Mason, M., Nelson, E., Nemeth, Z., Reynolds, D., Robson, H.
787 K., Roman-Gonzalez, A., Scherer, P., Scolding, J., Short, J., Wilkin, J. T. R., Wilson, D. R. (2022). DY150 Cruise report.
788 <https://seachange-erc.eu/research/north-west-european-research-cruise>
- 789 Sejrup, H. P., & Haugen, J. -E. (1994). Amino acid diagenesis in the marine bivalve *Arctica islandica* Linné from northwest
790 European sites: Only time and temperature? *Journal of Quaternary Science*, 9(4), 301–309.
791 <https://doi.org/10.1002/jqs.3390090402>
- 792 Stuiver, M., & Reimer, P.J. (1993): Extended ^{14}C data base and revised CALIB 3.0 ^{14}C age calibration program. *Radiocarbon*,
793 35, 215–230. doi:10.1017/S0033822200013904
- 794 Sykes, G. A., Collins, M. J., & Walton, D. I. (1995). The significance of a geochemically isolated intracrystalline organic
795 fraction within biominerals. *Organic Geochemistry*, 23(11–12), 1059–1065. [https://doi.org/10.1016/0146-6380\(95\)00086-0](https://doi.org/10.1016/0146-6380(95)00086-0)
- 796 Tomiak, P. J., Andersen, M. B., Hendy, E. J., Potter, E. K., Johnson, K. G., & Penkman, K. E. H. (2016). The role of skeletal
797 micro-architecture in diagenesis and dating of *Acropora palmata*. *Geochimica et Cosmochimica Acta*, 183, 153–175.
798 <https://doi.org/10.1016/j.gca.2016.03.030>
- 799 Tomiak, P. J., Penkman, K. E. H., Hendy, E. J., Demarchi, B., Murrells, S., Davis, S. A., McCullagh, P., & Collins, M. J.
800 (2013). Testing the limitations of artificial protein degradation kinetics using known-age massive *Porites* coral skeletons.
801 *Quaternary Geochronology*, 16, 87–109. <https://doi.org/10.1016/j.quageo.2012.07.001>
- 802 Torres, T., Ortiz, J. E., & Arribas, I. (2013). Variations in racemization/epimerization ratios and amino acid content of
803 *Glycymeris* shells in raised marine deposits in the Mediterranean. *Quaternary Geochronology*, 16, 35–49.
804 <https://doi.org/10.1016/j.quageo.2012.11.002>



- 805 Towe, K. M., & Thompson, G. R. (1972). The structure of some bivalve shell carbonates prepared by ion-beam thinning - A
806 comparison study. *Calcified Tissue Research*, 10, 38–48.
- 807 Trofimova, T., Milano, S., Andersson, C., Bonitz, F. G. W., & Schöne, B. R. (2018). Oxygen isotope composition of *Arctica*
808 *islandica* aragonite in the context of shell architectural organization: Implications for paleoclimate reconstructions.
809 *Geochemistry, Geophysics, Geosystems*, 19(2), 453–470. <https://doi.org/10.1002/2017GC007239>
- 810 Vallentyne JR. 1964. Biogeochemistry of organic matter II: Thermal reaction kinetics and transformation products of amino
811 compounds. *Geochimica et Cosmochimica Acta* 28:157-88
- 812 Walker, M., Head, M. J., Lowe, J., Berkelhammer, M., Björck, S., Cheng, H., Cwynar, L. C., Fisher, D., Gkinis, V., Long,
813 A., Newnham, R., Rasmussen, S. O., & Weiss, H. (2019). Subdividing the Holocene Series/Epoch: formalization of stages/ages
814 and subseries/subepochs, and designation of GSSPs and auxiliary stratotypes. *Journal of Quaternary Science*, 34(3), 173–186.
815 <https://doi.org/10.1002/jqs.3097>
- 816 Walton D. 1998. Degradation of intracrystalline proteins and amino acids in fossil brachiopods. *Organic Geochemistry* 28:389-
817 410
- 818 Wanamaker Jr., A. D., Butler, P. G., Scourse, J. D., Heinemeier, J., Eiríksson, J., Knudsen, K. L., & Richardson, C. A. (2012).
819 Surface changes in the North Atlantic meridional overturning circulation during the last millennium. *Nature Communications*,
820 3(899), 1–7. <https://doi.org/10.1038/ncomms1901>
- 821 Wheeler, L. J., Penkman, K. E. H., & Sejrup, H. P. (2021). Assessing the intra-crystalline approach to amino acid
822 geochronology of *Neogloboquadrina pachyderma* (sinistral). *Quaternary Geochronology*, 61(June 2020), 101131.
823 <https://doi.org/10.1016/j.quageo.2020.101131>
- 824 Witbaard, R., Duineveld, G. C. A., & de Wilde, P. A. W. J. (1997). A long-term growth record derived from *Arctica Islandica*
825 (Mollusca, Bivalvia) from the Fladen ground (northern North Sea). *Journal of the Marine Biological Association of the United*
826 *Kingdom*, 77(3), 801–816. <https://doi.org/10.1017/s0025315400036201>
827